



AALBORG UNIVERSITET

Maturation of Human Dendritic Cells upon Delivery of cGAMP

Aalborg University

Agnieszka Janina Banasik

31.05.2018

Project title:

Maturation of Human Dendritic Cells
upon Delivery of cGAMP

Paper submission date:

31st of May, 2018

Project period:

1st of September, 2017 – 20th of June, 2018

Group:

17gr9042

Author:

Agnieszka Janina Banasik

Supervisor:

Emil-Kofod Olsen

Co-Supervisors:

Ralf Agger

Laboratory of Immunology and Cancer Biology
Department of Health, Science and Technology
Aalborg University
Aalborg, Denmark

Project report:

Number of pages:

44

Number of appendices:

14

Acknowledgement:

I wish to thank member of the Laboratory of Immunology at Aalborg University Brita Serup Holst and my college Marlene Fyrstenberg Laursen for helpful guidance, assistance with laboratory work, and helpful discussions of results.

Special gratitude should be directed to my supervisor Emil Kofod-Olsen for excellent guidance and help with experiments introduces in the project.

Abstract

Activation of a host immune response against cancer cells is the main goal in cancer immunotherapy. Given that cancer cells evade the immune system, new strategies to activate the immune response are now under investigations. DAMPs, such as ATP, UAC and nuclear proteins, released from necroptotic cells, may evoke anti-tumor immune response. Moreover, recognition of cytosolic double stranded DNA (dsDNA) by the recently discovered mammalian enzyme cyclic GMP-AMP synthase (cGAS) induce production of non-canonical cyclic dinucleotide 2, 3'cGAMP. cGAMP directly binds to and activate the STING receptor leading to induction of type I interferons, mainly $INF\alpha$ and $INF\beta$.

The aim of this study was to investigate, whether cGAMP released from dead cells can mature moDCs *in vitro*.

To do that, cell death was induced in L929 cells using a combination of TNF/CHX or TNF/zVAD added to the cell culture. Dead cells, as well as supernatant from their cell culture induced maturation of moDCs based on up-regulation of cell surface markers CD80, CD86 and HLA-DR. Secondly, addition of caspases inhibitor zVAD-fmk to cell culture with immature DCs also triggered DCs activation, suggesting that necroptotic cells contribute to DCs activation. Further, we show that cGAMP can induce maturation in moDCs, and cGAMP triggered DCs maturation more potently than other DAMPs used at equivalent molar concentration. Lastly, we show that co-culture of PBMCs with cGAMP-matured DCs, resulted in PBMCs proliferation and increased levels of the cytokines IL-10, IL-1 β and $INF\gamma$ detected by multiplex assay MSD.

The observed results show that cGAMP can induce DCs maturation and may be one of the DAMPs released by necroptotic cells.

TABLE OF CONTENT

Abstract 2

1. The human immune system 5

 1.1 Dendritic cells as a key cellular component of the innate immunity 5

2. Cell Death. 7

 2.1 Apoptosis: characterisation based on morphological features. 7

 2.2 Necroptosis: morphological characteristics and proinflammatory responses due to release of DAMPs. 8

 2.3 Molecular mechanism and pathways leading to cell survival, apoptosis and necroptosis..... 8

 2.3.1 Cell survival dependent on complex I formation. 9

 2.3.2 Complex IIa formation and apoptosis pathway. 9

 2.3.3 Complex IIb- the necrosome signalling complex leading to necroptosis. 10

3. Importance of necroptosis in host defences..... 12

 3.1 Cytosolic DNA sensing via cGAS-cGAMP-STING axis. 12

4. Materials and methods. 14

 4.1 Culturing of mouse *L929 cells* and human *HT-29 cells* 14

 4.1.1 Cell death induction in L929 and HT-29 cells 14

 4.1.2 Cell lysis for protein extraction..... 14

 4.2 PBMCs purification, in-vitro generation of DCs from monocytes and cells culturing 14

 4.2.1 Maturation of human monocyte- derived dendritic cells (moDCs) 15

 4.3 Mixed Leukocyte Reaction (MLR). PBMCs staining for proliferation assay. 15

 4.3.1 Cytokines detection and quantification using electro-chemiluminescence-based Mesoscale Discovery (MSD) Multiplex Assay 15

 4.4 Cells morphology observation and imaging 17

 4.5 Cell death assay by flow cytometry..... 17

 4.6 Dendritic cells (DCs) surface-marker expression: staining and analysis by flow cytometry. 17

 4.7 Staining of PBMCs for T cells population..... 18

5. Results 19

 5.1 L929 cells die upon treatment with combination of TNF+ CHX or TNF+ zVAD 19

 5.2 Cells dying by necroptosis contributes to maturation of DCs *in vitro* 20

 5.3 Supernatant collected from dead L929 cells mature DCs 20

5.4 cGAMP matures Dendritic Cells <i>in vitro</i>	21
5.5 cGAMP matures Dendritic Cells more potent than ATP and Uric Acid Crystals.....	24
5.6 Co-culture of T cells with cGAMP-matured DCs resulted in T cells proliferation and increased levels of the cytokines: IL-10, IL-1 β and INF γ detected by multiplex assay MSD.....	24
6. Discussion	27
7. Conclusion	29
8. Future prospects.....	30
Bibliography.....	42

1. The human immune system

The human immune system comprises of a complex of interrelated physiological mechanisms designed primarily to serve as a line of defence against pathogens (infectious microorganisms). The multiphasic role of the immune system consists of organism recognition, evaluation and response. It develops over lifetime, agglomerating a database of cellular and endocrine responses to specific stimuli that it has been exposed to, aiming to equilibrate the body back to its pre-stimulated form. The system itself has two main functional derivatives – the innate immune system and the adaptive immune system. The former is responsible for the non-adaptive responses. Innate immune system is a collective of mechanisms adapted through evolution and is naturally present in a vast majority of multicellular organisms. It induces the first line of defence against pathogens and other invasive agents, aiming to maintain the body's physiological *status quo*. The adaptive immune system is vertebrate specific and bears the role of conducting the advanced defence operations. It is capable of forming the immunological memory that stores the recollections of the previously contacted pathogens, and the strategies once used to defeat them.

1.1 Dendritic cells as a key cellular component of the innate immunity

The innate (natural) immune system consist of phagocytic cells, such as neutrophils, macrophages (derived from blood-borne monocytes) and dendritic cells (DCs) that endocytose extracellular antigens and present them to T cells. Dendritic cells are the most potent antigen presenting cells (APCs) in the immune system. Most of the DCs originate directly from myeloid stem cells in the bone marrow, whereas other DCs derive from monocytes. DCs express many cell surface receptors, which upon ligation with antigen contributes to maturation of a DCs. An example being Pathogen-Associated Molecular Patterns (PAMPs), which are expressed by different pathogens infecting the organism e.g. Lipopolysaccharide (LPS) or Damage-Associated Molecular Patterns (DAMPs), which report about cell damage or death (Ebrahimi *et al.*, 2009).

Upon activation, dendritic cells up-regulate the expression of CD28, CD80 and CD86 molecules on their cell surface, important for the signals and activation of lymphocytes, particularly not previously stimulated-naïve T cells. The antigen is processed intracellularly into short peptides by means of proteolytic cleavage before it is presented by major-histocompatibility-complex (MHC) molecules on the surface of dendritic cells (Mackay *et al.*, 2000). There are two classes of MHC molecules: class I, which present the peptides to the T-cell receptor (TCR) found on the surface of cytotoxic T cells, and class II molecules, which present the peptides to the TCR found on the surface of helper T cells.

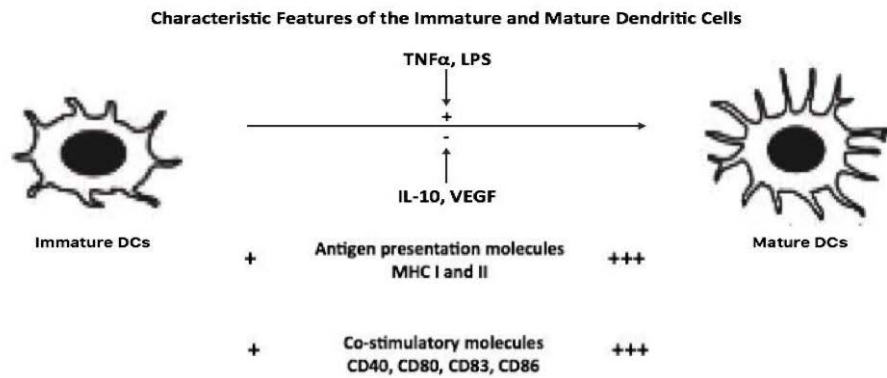


Figure 1 Distinctive features of Immature and Mature DCs. The level of cell surface expression of molecules: CD40, CD80, CD83, CD86 as well as MHC I and MHC II allow to distinguish immature DCs from mature DCs. Tumour Necrosis Factor alpha (TNF α) and Lipopolysaccharide (LPS) are known to induce DCs maturation. Interleukin (IL) 10 and Vascular Endothelial Growth Factor (VEGF) have a negative effect on the maturation of dendritic cells (DCs).

2. Cell Death.

In the human body cells die in a controlled way- a process known as programmed cell death. This is one of the mechanisms to eliminate unwanted cells and cell divisions together with many regulatory pathways balance the cell death in healthy individuals. Programmed cell death usually, but not exclusively, occurs by apoptosis, which so far is the best known and most common form. Necroptosis, pyroptosis and ferroptosis are non-apoptotic forms of programmed cell death, which have been recently described.

In the case of injury or trauma, an accidental and a passive form of cell death, known as necrosis, occurs as a result of physicochemical injury or viral and bacterial infections (Moreno-Gonzalez, Vandenabeele and Krysko, 2016). However, identification of signalling molecules in necrotic cell death i.e. receptor interacting protein kinase 1 (RIPK1) and RIPK3 kinase raised the concept of necrotic cell death as a genetically controlled cell death. Since then, in order to distinguish programmed necrosis from accidental necrosis, the term necroptosis was introduced (Moreno-Gonzalez, Vandenabeele and Krysko, 2016).

The immune system carefully balances its response to dead and dying cells, that is to prevent the development of autoimmunity and hence to maintain homeostasis. However, even though the uptake and clearance of dying cells is a tolerogenic process, dying cells can also emit damage-associated molecular patterns (DAMPs), depending on the nature of the cells death (Klarquist *et al.*, 2014).

2.1 Apoptosis: characterisation based on morphological features.

Rounding and shrinking of the cells (pyknosis), chromatin condensation, DNA fragmentation, nuclear fragmentation (karyorrhexis) and plasma membrane blebbing are all hallmarks of programmed cell death referred to as apoptosis (Figure 2)

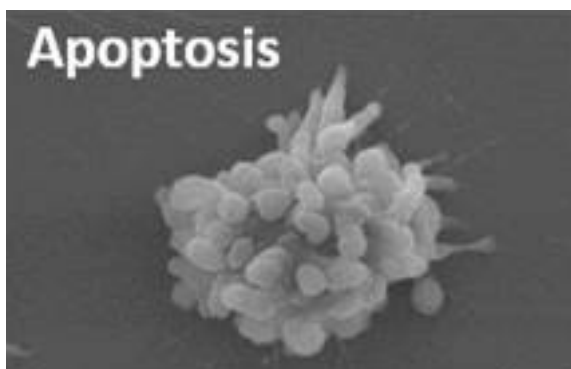


Figure 2 Representation of plasma membrane blebbing- one of the main morphological characteristics of cell undergoing apoptosis. Picture was captured by (Chen *et al.*, 2016)

In order to avoid the contact of nuclear remnants with the immune system, apoptotic cell chromatin is degraded by internal proteases (called caspases) and nucleases before the cells lose their membrane integrity. Plasma membrane proteins together with mitochondrial proteins are further cleaved by “executioner” caspases, ultimately leading to cell death. Thus, activity of caspases is

another characteristic feature of apoptosis. The apoptotic bodies, which are membrane-wrapped vesicles containing fragments of cytoplasmic organelles, are further phagocytosed by macrophages and therefore this death process does not evoke immune response, as endogenous molecules are not released into the extracellular environment, as opposed to a necroptotic cell death (Chen and Nuñez, 2010).

2.2 Necroptosis: morphological characteristics and proinflammatory responses due to release of DAMPs.

Cellular rounding and swelling of the cells (oncosis) due to disruption of osmotic balance within the dying cell, loss of plasma membrane integrity and, most importantly, cell rupture- leading to release of (DAMPs) are typical morphological and biochemical features of necroptotic cells. Another characteristic feature is the absence of caspase activity (Cho, Challa and Chan, 2011; Moreno-Gonzalez, Vandenabeele and Krysko, 2016).

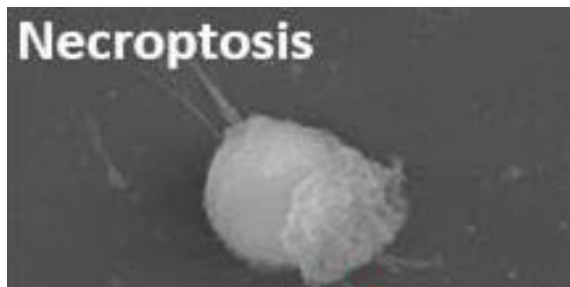


Figure 3 Necroptotic cell. Picture taken by (Chen et al., 2016) represents rupture of the cell membrane, a main feature of cells undergoing necroptosis.

The best characterised intracellular DAMPs are: chromatin-associated protein high-mobility group box 1(HMGB1), heat shock proteins (HSPs) (e.g. HSP70 present in cytosol and nucleus), purine metabolites i.e. ATP and uric acid (UCA) (Moreno-Gonzalez, Vandenabeele and Krysko, 2016).

2.3 Molecular mechanism and pathways leading to cell survival, apoptosis and necroptosis.

Apoptosis can be triggered via extrinsic or intrinsic pathways. The first one depends on external stimulus, such as DAMPs or cytokines, which bind to and activate “death receptors”, whereas the intrinsic pathway is triggered by stimuli from inside the cells, such as damaged DNA or oxidative stress.

Below, the example of extrinsic pathway triggered by a soluble molecule tumour necrosis factor alpha (TNF α) will be described. TNF α binding can result in cell survival, apoptosis or necroptosis, depending on signals that operate downstream of TNF receptor 1 (TNFR1) (Vandenabeele *et al.*, 2010).

2.3.1 Cell survival dependent on complex I formation.

TNF α is produced by activated macrophages. Once TNF α binds the extracellular site of death receptor TNFR1, located on the cell surface, changes in the intracellular portion of TNFR1 leads to recruitment of a receptor associated complex I, which further triggers downstream signalling. This complex comprises of TNF-receptor-associated death domain (TRADD) and receptor interaction protein kinase 1 (RIPK1), which is polyubiquitinated by TNF α receptor associated factor 2/5 (TRAF 2/5) and cellular inhibitor of apoptosis proteins (cIAPs) **at the position of lysine 63**. Ubiquitinated RIPK1 serves as a scaffold for the recruitment of transforming growth factor- β activated kinase 1 (TAK1), TAK1-binding protein 2 (TAB2) and TAB3, which promote cell survival through activation of nuclear factor kappa B (NF- κ B) pathway and mitogen-activated protein kinase (MAPK) pathway (Figure 4A).

However, successive deubiquitination of RIPK1 leads to dissociation of RIPK1, resulting in formation of complex IIa (known as death inducing signalling complex (DISC)) or complex IIb (necrosome complex), both promoting cell death- apoptosis or necroptosis, respectively (Vandenabeele *et al.*, 2010; Wu, Liu and Li, 2012).

2.3.2 Complex IIa formation and apoptosis pathway.

Two proteins are known to take part in RIPK1 deubiquitination: cylindromatosis (CYLD) and A20 enzyme (also known as tumour necrosis factor, alpha-induced protein 3 (TNFAIP3)), both negatively regulating NF- κ B pathway. CYLD is encoded by a tumour suppressor gene and inhibits NF- κ B pro-survival pathway by cleaving Lys⁶³-linked polyubiquitin chains from several proteins. A20 triggers proteasome-dependent degradation of E3 ligases i.e. TRAF2 and cIAPs from Lys⁶³. As a result, deubiquitinated RIPK1 is released from complex I to the cytoplasm and forms complex IIa. RIPK1(deubiquitinated) form complex IIa with TRADD, which then recruit several molecules of procaspases (Vandenabeele *et al.*, 2010; Wu, Liu and Li, 2012). These procaspases, located now in a close proximity to each other, become activated by self-cleavage, as procaspases have low enzymatic activity. This results in activation of so called “initiator” caspases (caspase -2, -8, -9 and -10), which further trigger cascade of caspase activation and formation of “executioner” caspases (caspase-3, -6, and -7). These executor caspases lead to mass proteolysis of nuclear, plasma membrane and mitochondrial proteins, causing the cells to break into apoptotic bodies and ultimately leading to cell death- apoptosis (Pecorino, 2012) (Figure 4 B). Moreover, caspase-8 inactivate RIPK1 by proteolytic cleavage, which deprives its activity and therefore abrogates the stimulatory role of RIPK1 in the activation of NF- κ B pro-survival pathway (Moreno-Gonzalez, Vandenabeele and Krysko, 2016).

By contrast, when caspase-8 is blocked or deleted, complex II cannot enter the “apoptotic mode” and TNFR1 ligation results, in most of the cases, in necroptosis (Vandenabeele *et al.*, 2010).

2.3.3 Complex IIb- the necrosome signalling complex leading to necroptosis.

Necroptosis is dependent on activation of receptor-interacting kinase 3(RIPK3) and the mixed lineage kinase domain-like (MLKL) pseudokinase (Vanden Berghe *et al.*, 2015). Necrosome refers to a multiprotein complex that is composed of TRADD, RIPK1, RIPK3, and which is assembled when caspase 8 is inhibited or deleted. In complex IIb, RIPK1 recruits RIPK3 and their direct interaction is maintained via mutual phosphorylation at RIP homotypic interaction motifs (RHIM), which is required to guarantee the activation of necroptosis pathway. Activated RIPK3 phosphorylates MLKL at threonine 357 and serine 358, which next multimerizes and translocate to the plasma membrane, where it binds to phosphatidylinositol lipids and cardiolipin, ultimately leading to membrane permeabilization and induction of necroptotic cell death, although the mechanism is incompletely understood (Figure 2C) (Wu, Liu and Li, 2012; Vanden Berghe *et al.*, 2015).

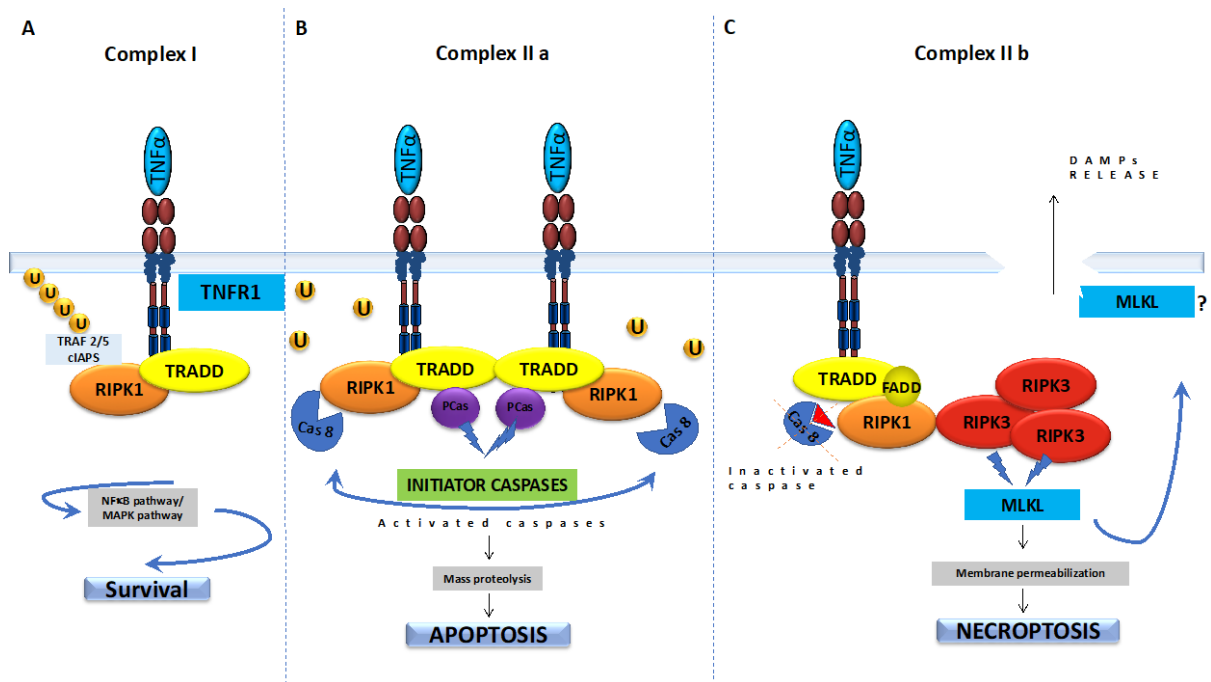


Figure 4 An overview of Complex I, Complex IIA and Complex IIb formation.

Stimulation with tumour necrosis factor α (TNF α) results in recruitment of TNF receptor 1 (TNFR1)-associated death domain protein (TRADD) and receptor-interacting protein kinase 1 (RIPK1). E3 ubiquitin ligase TNFR-associated factor 2/5 (TRAF2/5) are recruited together with cellular inhibitor of apoptosis (cIAP) 1 and 2 to TRAF2/5, before cIAPs place different lysine-linked ubiquitin chains on various components of the TNFR signalling complex. Complex I activates NF κ B and MAPK pathways, which facilitate cell survival(A). In sensitized cells (e.g., stimulated with TNF and cycloheximide (CHX)), the cytoplasmic complex IIa is formed consisting of: TRADD, deubiquitinated RIPK1 and active caspases-8, which leads to apoptosis (B). Formation of the necrosome (TRADD, FADD, RIPK1, RIPK3, and mixed lineage kinase domain-like [MLKL]) also called Complex IIb, leads to necroptosis when

caspase-8 is inhibited. In the case of TNF, activated RIPK1 recruits RIPK3 via RHIM–RHIM domain interactions, resulting in phosphorylation of RIPK3 and MLKL. On phosphorylation, MLKL oligomerizes and translocates to the plasma membrane, where it causes lysis and release of damage-associated molecular patterns (DAMPs) (C).

Evidences demonstrate that RIPK3 is crucial in triggering necroptosis, as knockdown of RIPK3 or low expression levels of RIPK3 notably inhibits cells ability to undergo necroptosis and transfection of this cells with the RIPK3 gene enables them to undergo necroptosis when the apoptotic pathway is blocked (He *et al.*, 2009; Cho, Challa and Chan, 2011). Indeed, suppression of apoptosis may drive cells to undergo necroptosis as an alternative cell death mechanism and this can be achieved by using caspases inhibitors such as zVAD-fmk. Nonetheless, the presence of exogenous TNF α is required to trigger necroptosis. The importance of phosphorylation between RIPK1 and RIPK3 in triggering necroptosis is indicated by inhibiting RIPK1 kinase activity with Necrostatin-1, which results in abolished TNF-induced RIPK3 recruitment as well as RIPK1/RIPK3 interactions under pro-necrotic stimulation (TNF+zVAD-fmk). Thus, Necrostatin-1 is known to inhibit complex II formation (Cho, Challa and Chan, 2011).

3. Importance of necroptosis in host defences.

Many viruses encode caspase- or apoptosisinhibitors, viral infections may drive the cell death response towards necroptosis (Cho, Challa and Chan, 2011). It could be possible that necroptosis serves as an alternative death route in the case of a defect in the first-line cell death response (apoptosis). Therefore, necroptosis might be a back-up mechanism, which evolved in order to eliminate infected cells with virus and hence to promote inflammation through release of DAMPs from necroptotic cells.

One of the important mechanism of the innate immune system is to sense the presence of nucleic acid of self or foreign origin, particularly because it is present in viruses, bacteria, (Lee and Barton, 2014). Recognition of cytosolic host DNA, derived from nuclear or mitochondrial leakage following cell division or as a consequence of DNA damage is executed by the same receptors (Barber, 2015). Without any doubt, presence of the DNA in the cytoplasm is a danger signal that drives host immune responses and triggers type I interferon pathway. Production of type I interferons (IFNs) triggers host immune cells to defend against viruses, bacteria, parasites and fungi. So far, it was known that microbial derived nucleic acid is recognised by most endosomal TLRs and that DNA can activate production of type I IFNs in dendritic cells via binding to TLR9 ligands in endosomes, reviewed by Bettina Lee *et al.*, 2014 (Lee and Barton, 2014). Recently, the study of Sun *et al.*, 2013 identified a mammalian cytosolic DNA sensor- cGAS that induces type I interferons by producing soluble second messenger cGAMP (Sun *et al.*, 2013).

3.1 Cytosolic DNA sensing via cGAS-cGAMP-STING axis.

The recently discovered mammalian enzyme cyclic GMP-AMP synthase (cGAS) upon recognition of a double stranded DNA (dsDNA), catalyses ATP and GTP into non-canonical cyclic dinucleotide 2',3'cGAMP (Ahn *et al.*, 2012; Sun *et al.*, 2013; Ng *et al.*, 2018). cGAMP, a soluble second messenger, directly binds to and activate the adaptor protein stimulator of interferon genes (STING; also known as *Tmem 173*), which is a 379 amino acid transmembrane protein. STING resides as a dimer in the endoplasmic reticulum (ER) membrane of epithelial and endothelial cells, as well as hematopoietic cells such as macrophages and dendritic cells (Ishikawa, Ma and Barber, 2009; Ahn and Barber, 2014; Barber, 2015). Activation of STING leads to conformational changes at STING residues, which results in recruitment of cytosolic kinases: I kappa β (IKK) and TANK-binding kinase 1 (TBK1), which are key elements of proinflammatory signalling. These kinases together with STING are then relocated from ER to perinuclear regions of the cell, where IKK and TBK1 activate NF- κ B and IFN regulatory factor 3 (IRF3) transcription factors, respectively. Activated NF- κ B and IRF3 enter the nucleus and induce production of type I interferons, mainly INF α and INF β (Figure 5) (Saitoh *et al.*, 2009; Wu *et al.*, 2013; Barber, 2015).

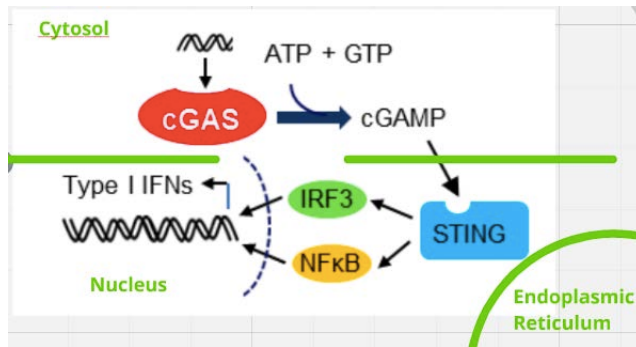


Figure 5 Cytosolic DNA recognition via cGAS-cGAMP-STING pathway. DNA recognition is triggered in an indirect fashion that depends on the enzyme cGAS, which upon interaction with DNA, synthesizes cGAMP that in turn binds to and activates STING. STING is located on the endoplasmic reticulum (ER) and is essential for controlling the transcription of numerous host defence genes, including type I interferons (IFNs) and pro-inflammatory cytokines.

It was shown that mammalian cGAMP is more potent in inducing type I IFNs than other cyclic dinucleotides, such as c-di-AMP, c-di-GMP or canonical 3'3'-cGAMP produced by bacteria (Wu et al., 2013). What makes cGAMP different from a normal protein- receptor binding is that cGAMP is a secondary soluble messenger, which binds to and activate STING receptor. Moreover, it can be transferred from producing cells to neighbouring cells through gap junctions, where it promotes STING activation and thus proinflammatory immunity (Ablasser et al., 2013). The question arised, whether cGAMP may be one of the DAMPs released from the cells following non-apoptotic cell death, such as necroptosis. In chemotherapy and radiotherapy models, treated cancers cells were shown to release DAMPs like ATP or HMGB1 and activate DCs via TLRs, which in turn contributed to induction of antitumor T cells. These data indicate that tumour cell-derived factors can facilitate induction of antitumor immunity (Woo et al., 2014). Furthermore, the study of Woo et al., 2014 shows that the only tumour-derived molecule that could induce IFN I production was DNA, which was mediated through cGAS, STING, and IRF3, and that the spontaneous T cells priming appears to be dependent on host type I IFN production. Moreover, Reboulet *et al.*, 2011 indicated that DCs upon phagocytosis of dead cells produce type I IFNs (Reboulet *et al.*, 2010). Because evidence shows that type I IFNs are required for antitumor CD8+ T cells responses (Diamond et al., 2011; Fuertes et al., 2011), and that cytosolic accumulation of DNA is observed in cancer cells, it would be interesting not only to trigger non-apoptotic death in cancer cells in order to release the intracellular “adjuvants” into extracellular space but also to determine if other intracellular components, released from dying cells, may contribute to STING activation and IFN I production.

In this report, we are going to investigate the maturation status of DCs upon exposure to dead and dying cancer cells and compare with cGAMP- stimulated DCs. We are also going to examine whether cGAMP can stimulate DCs activation better than other molecules, such as ATP or UAC, and finally to identify whether cGAMP could be one of the DAMPs released by non-apoptotic dead cells.

4. Materials and methods.

4.1 Culturing of mouse *L929 cells* and human *HT-29 cells*

Mouse L929 fibroblastic cell line was obtained from Søren Riis Paludan, Aarhus University, and human colorectal adenocarcinoma HT-29 cell line was a gift from Svend Birkelund, Aalborg University.

L929 and HT-29 cells were taken from -140°C freezer, thawed and cultured in DMEM (1X) medium (Gibco™) supplemented with 2mM L-glutamine and 10% FBS (Thermo Fisher Scientific) in 75cm² cell culture flask (T-75) (Greiner Bio-One). Cells were incubated at 37°C, 20 % O₂, 5 % CO₂ until reaching a confluence around 80% (approx. 7.5×10^6 cells in T-75 culture flask). Cells were checked every day using inverted phase contrast microscope (Leica DMIL) and the fully supplemented medium was changed every third day.

When cells reached the confluence of 80%, medium from the cells was discarded and cells were rinsed with PBS (Amresco) and de-attached from culture flask using trypsin/EDTA in PBS (2.5% and 0.5mM). Trypsinisation was terminated within 5 min of incubation at 37 °C, 20 % O₂, 5 % CO₂ by addition of fully supplemented warm DMEM (1X) medium (Gibco™) into the culture flask. Then, de-attached cells were harvested from the culture flask, counted in a hemocytometer and seeded on a 12 well cell culture plates (Greiner Bio-One) at density 0.4×10^6 cells per well. Cells were cultured in a fully supplemented DMEM (1X) medium (Gibco™).

4.1.1 Cell death induction in *L929* and *HT-29* cells

Cell death was induced by treating L929 or HT-29 cells with various combinations of 10ng/mL human tumour necrosis factor-alpha (TNF α) (Sigma Aldrich), 10 μ M cycloheximide (CHX) (Sigma Aldrich), and 10 μ M zVAD-fmk (InvivoGen). Cells were incubated at 37 °C, 20 % O₂, 5 % CO₂.

4.1.2 Cell lysis for protein extraction

L929 and HT-29 cells have been washed in PBS (Amresco) and de-attached from the bottom of the well using trypsin/EDTA in PBS (2.5% and 0.5mM). Trypsinisation was terminated within 5 min of incubation at 37 °C, 20 % O₂, 5 % CO₂ by addition of fully supplemented warm DMEM (1X) medium (Gibco™) to each well. De-attached cells have been transferred to sterile 2.0mL microcentrifuge tubes (Thermo Scientific) and washed in cold PBS (Amresco). A mixture of 10x lysis buffer (Cell Signalling Technology) and 10x complete mini protease inhibitor (Roche) in proportion 1:1 have been added to washed cells and the cells were incubated for 30 min on ice. After incubation time, cells were centrifuged at 5000g, 4 °C, acc. 6, break 2 for 10 min. Then, the lysate has been carefully collected, transferred to new sterile 2.0mL microcentrifuge tubes, followed by another centrifugation at 14000g, 4 °C, acc. 6, break 2 for 15 min. The lysate has been carefully collected avoiding remaining cells pellet on the bottom of the microcentrifuge tubes.

4.2 PBMCs purification, in-vitro generation of DCs from monocytes and cells culturing

Peripheral blood was collected in 7.5 mL sodium-heparin S-Monovette tubes (Sarstedt) from a known healthy donor and diluted 1:1 in RPMI 1640 medium (Invitrogen). Peripheral blood mononuclear cells (PBMCs) were purified using gradient density centrifugation with lymphoprep (Medinor). Then,

monocytes were extracted from PBMCs by a negative selection using Human Monocyte Isolation Kit II (Miltenyi Biotech). After isolation, monocytes were seeded on a 12 well culture plate (Greiner Bio-One) at density approximately 520.000 monocytes per well. The cells were cultured in RPMI 1640 medium (Invitrogen) supplemented with 10% FBS (Thermo Fisher Scientific), 100 U/ml penicillin, 100µg/ml streptomycin (Sigma-Aldrich), 2mL L-glutamine, 400 U/ml IL-4 and 1000 U/ml GM-CSF (Miltenyi Biotech) and incubated at 37 °C, 20 % O₂, 5 % CO for six days. On day three of moDCs incubation time, fully supplemented medium, as previously described, was added to cells.

4.2.1 Maturation of human monocyte- derived dendritic cells (moDCs)

DCs were matured using 10ng/mL lipopolysaccharide (LPS) (Sigma Aldrich), 10µM zVAD-fmk (InvivoGen), 100µl of supernatant collected from dead L929 cells, different concentrations of 2'3'-cGAMP (InvivoGen): 0.2µM, 2µM, 20µM, 100 µM; 100µM of Adenosine 5'-triphosphate disodium salt hydrate (ATP) (Sigma Aldrich), 100 µM Uric Acid Crystals (UAC) (Sigma Aldrich).

4.3 Mixed Leukocyte Reaction (MLR). PBMCs staining for proliferation assay.

Full blood was collected in 7.5 mL sodium-heparin tubes (S-Monovette) from a healthy donor 2 and diluted 1:1 in RPMI 1640 medium (Invitrogen). PBMCs were purified using gradient density centrifugation with lymphoprep (Medinor) and harvested from the interphase using Pasteur pipette. Purified PBMCs have been further washed in PBS, following staining with eFluor 670 (eBioscience) for cells proliferation assay. Stained PBMCs were incubated for 10 min at 37 °C, 20 % O₂, 5 % CO₂ and the incubation was terminated by addition of cold medium to cells, followed by incubation on ice for 5 min. The cells were washed in fully supplemented medium and added to cGAMP-treated moDCs in approximately 1:1 proportion. The cells were co-cultured for four days at 37 °C, 20 % O₂, 5 % CO₂.

4.3.1 Cytokines detection and quantification using electro-chemiluminescence-based Mesoscale Discovery (MSD) Multiplex Assay

The principle of the MSD assay is based on the formation of a “sandwich” complex just like in a traditionally used enzyme-linked immunosorbent assay (ELISA), where a capture antibody, immobilized on the surface of the plate, binds to the protein of interest, which is further detected by a secondary antibody conjugated to a label that emits light when is excited. The foundation that makes MSD a “multiplex assay” is the design of a detection plate, called MULTI-SPOT[®] U-PLEX, which enables to quantify up to 10 analyses per well from a single sample, thereby minimising sample volume required for analysis, time and costs of the assay as compared to traditional single-plex ELISA assay.

For the detection and quantification of cytokines in the serum collected from the MLR experiment, the human TH1/TH2 Combo sector kit (cat no. K15010K-1) was used, which measures the cytokine levels of: IFN-γ, IL-1β, IL-2, IL-4, IL-5, IL-8, IL-10, IL-12p70, IL-13, and TNF-α on a 10-spot 96-well U-PLEX plate.

First of all, each biotinylated capture antibody: human IFN_γ, IL-1β, IL-2, IL-4, IL-5, IL-8, IL-10, IL12P70, IL-13 and TNF-α was coupled to its assigned U-plex Linker.

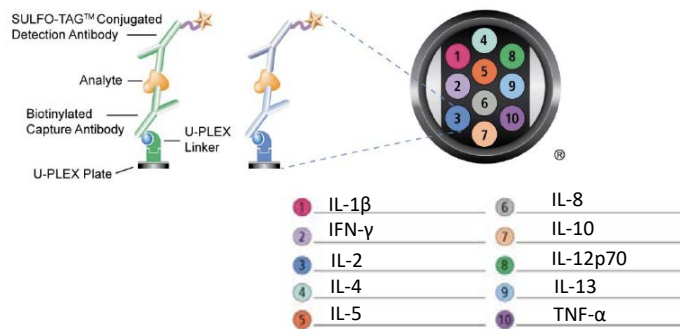


Figure 6 Visualisation of a 10-spot well designed for multiplex assay.

The principle of the Linker is that it works as a “key”, which fits to only one “locker” located on the bottom of each well of a U-PLEX plate. In this way, the biotinylated capture antibody is allocated on a specific location in the well (Figure 6). For a 10-spot 96-well plate, 10 different Linkers were provided. In order to assemble Linker with a capture antibody, these two “ingredients” were mixed together in proportion 3:2 in a sterile 2.0mL microcentrifuge tubes (Thermo Scientific) and left for 30 min incubation at RT, followed by addition of “Stop solution”. Next, all self- assembled Linker-antibody complexes were pooled together in a 15ml centrifuge tube (LabSolute) and applied to each well on a U-PLEX plate. The plate was then sealed with an adhesive plate seal and incubated with shaking at RT for 1 hour. During that time, calibration standards were prepared. Also, the cell supernatant samples were diluted 10x in Diluent 43.

After 1-hour incubation time, the plate was washed tree times in PBS plus 0.05% Tween-20 followed by addition of calibrator standards and samples: undiluted and diluted 10x. The plate was sealed with an adhesive plate seal and incubated with shaking at RT for 1 hour. At this stage, analyses were bound to its capture antibody immobilized in the well (Figure 6).

During the incubation time, SULFO-TAG™ Conjugated Detection Antibodies provided in the kit were diluted 100x in Diulent 3 and pooled together in one tube. After the incubation time, the plate was washed tree times PBS plus 0.05% Tween-20 and the pooled together SULFO-TAG™ Conjugated Detection Antibodies were added to each well. The plate was sealed with an adhesive plate seal and incubated with shaking at RT for 1 hour. After the incubation time, the plate was washed tree times PBS plus 0.05% Tween-20. Finally, 2x Read Buffer T was added to each well in order to provide the appropriate chemical environment for the electrochemiluminescence reaction. Once the plate was loaded on MSD instrument, the electrochemical stimulation at the electrode surface of the U-PLEX plate caused SULFO-TAG™ labels on Detection Antibodies to emit the light at 620 nm. The instrument measures the intensity of emitted light, which is proportional to the amount of analyse present in the sample. The results were analysed using Excel and Prism 6.

4.4 Cells morphology observation and imaging

The morphological changes have been observed under the inverted phase contrast microscope and the pictures were captured with microscope camera Axiocam ERc 5s (Zeiss) (PrimoVert, Zeiss).

4.5 Cell death assay by flow cytometry

Cells were harvested from the culture plate and transferred into 5ml polystyrene round-bottom tubes (BD Falcon™), followed by washing in PBS (Amresco) and staining with Fixable Viability Dye eFluor 780 (eBioscience), LIVE/DEAD staining. After 30 min incubation time in dark, cells were washed in PBS, followed by washing in flow buffer containing 0,1% BSA and 0.01% sodium azide (Sigma Aldrich). The stained cells were then checked for cells viability status using a CytoFlex S2 flow cytometer (Beckman Coulter). Data was analyzed in Kaluza software (Beckman Coulter) and Prism 6. The example of gating strategy is shown in Figure x

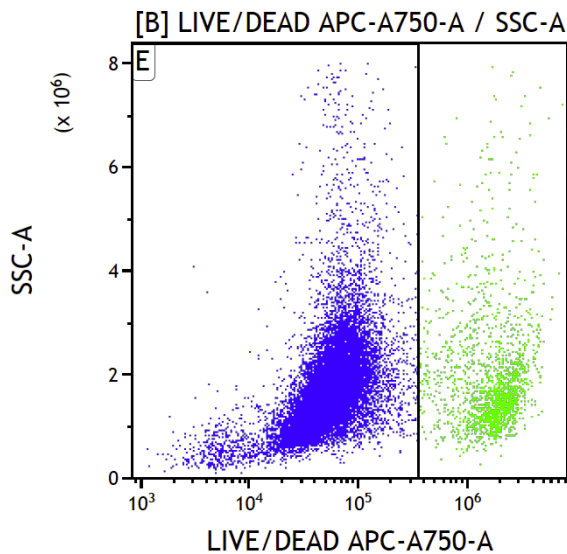


Figure 7 Example of gating strategy used for all samples during data analysis. A dot plot: side scatter area (SSC-A) versus LIVE/ DEAD APC-A750 area was created, in order to distinguish live and dead cell populations. Each dot on the graph represents one or more individual cells detected by a laser. Cells have been separated based on the eFlour 780 intensity, which is indicated on X-axis. The more cell membrane is ruptured, the higher the signal intensity of eFlour 780 staining. Cells indicated in blue have been gated as live, whereas cells indicated in green colour, have been gated as dead cells.

4.6 Dendritic cells (DCs) surface-marker expression: staining and analysis by flow cytometry.

Dendritic cells were harvested on day seven, washed in PBS and in flow buffer containing 0,1% BSA and 0.01% sodium azide (Sigma Aldrich). Next, cells were stained for expression of maturation markers with antibodies: mouse IgG1 κ anti-human CD83 PE-Cy7 (BD Bioscience), mouse IgG1 κ anti-

human CD86 BV421 (BD Bioscience) and mouse IgG1 κ anti-human HLA-DR- PE (R&D System). Relevant isotopes controls were included. The stained cells were analyzed using a CytoFlex S2 flow cytometer (Beckman Coulter) and minimum 10.000 events were recorded for each sample. Data was further analyzed in Kaluza software (Beckman Coulter) and Prism 6.

When analysing flow cytometry results in Kaluza software, the first step was to identify DCs population among other cell types. That was done by creating a dot plot: side scatter area (SSC-A) versus forward size area FSC-A (Figure 8A). Single cells were obtained by gating forward scatter height (FSC-H) versus forward scatter area (FSC-A) (Figure 8 B). Live cells were selected based on eFluor 780 intensity. To do that, the dot plot was created (SSC-A) versus LIVE/ DEAD APC-A750 area. Finally, the histograms were created to determine the median fluorescence intensity of each cell surface marker detected on gated cells.

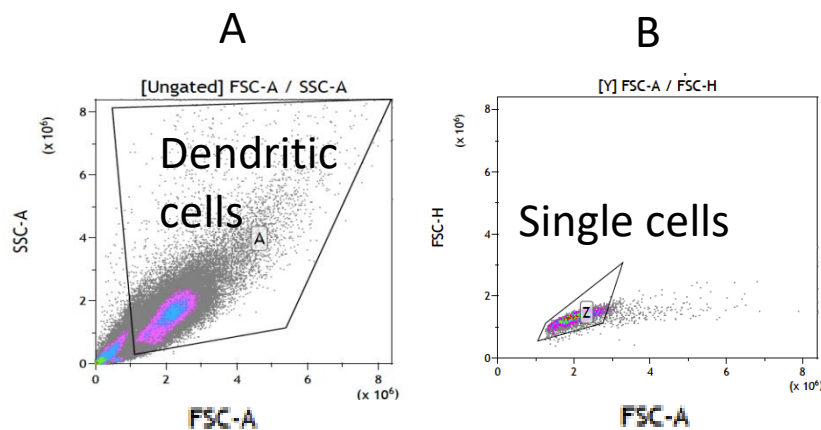


Figure 8 (A&B) Each dot on the graph represents one or more individual cells detected by a laser. The density of events on the plot is color-coded, with red representing the highest number of events, while green, blue violet and grey represent progressively lower event densities.

4.7 Staining of PBMCs for T cells population

PBMCs were stained for T cells characteristic markers; CD4 anti-human PerCP (clone OKT4) (BioLegend) and mouse anti-human CD8 Per-CP-Cy5.5TM (clone SK-1;CD8 α specific)(BD Biosciences). Gating method is included in Appendix 13.

5. Results

5.1 L929 cells die upon treatment with combination of TNF+ CHX or TNF+ zVAD

Firstly, I wanted to determine, whether L929 cells and HT-29 cells could die by apoptosis -upon the treatment with TNF+ CHX or by necroptosis- upon the treatment with TNF+ zVAD. To do that, I seeded the cells at density 0.4×10^6 cells per well on a 12-well culture plate. Then I added various combinations of 10ng/mL (TNF α), 10 μ M (CHX) and 10 μ M zVAD-fmk and the treated cells were left for incubation time either for 4 or 11 hours. The cells were stained with LIVE/DEAD staining and analysed by microscopy and flow cytometry. Below, selectively chosen pictures of the best interest have been presented, whereas full overview of each control is included in Appendix 2. Cell death was only observed in L929 cells, whereas high cell viability % was observed in HT-29 cells treated even up to 103 hours (Appendix 1). In Figure 9 A, we can see structures looking alike the apoptotic bodies, which seems to be released from the cells pointed with a blue arrow. The nucleus seems to be condensed and the cells are rounding-up. In Figure 9B, a blue arrow is pointing at the cell, which seems to be releasing intracellular components. From the flow cytometry results, we can see that TNF/zVAD killed L929 cells the most efficiently (Figure 9 C).

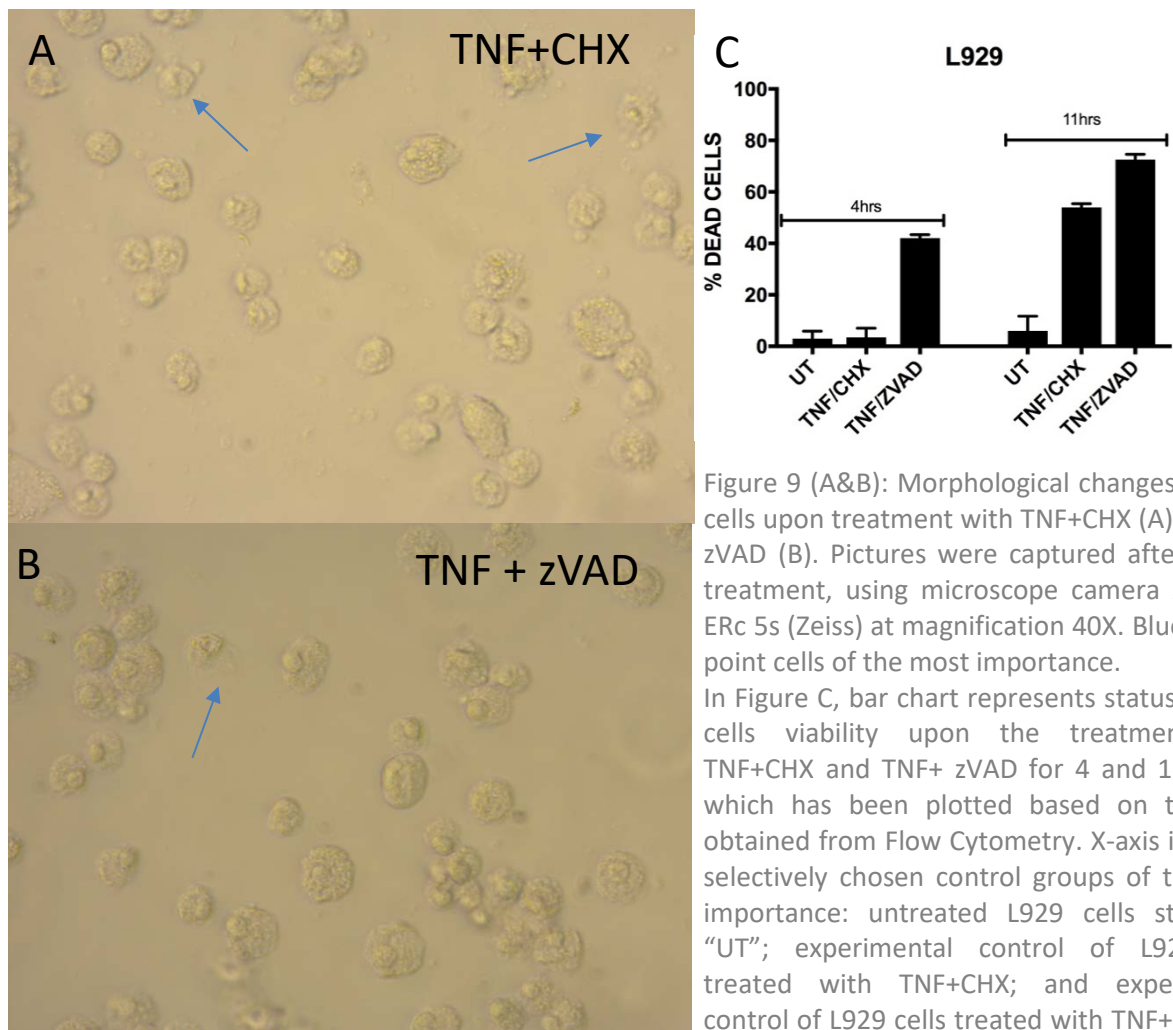


Figure 9 (A&B): Morphological changes of L929 cells upon treatment with TNF+CHX (A) or TNF+ zVAD (B). Pictures were captured after 11 hrs treatment, using microscope camera Axiocam ERc 5s (Zeiss) at magnification 40X. Blue arrows point cells of the most importance.

In Figure C, bar chart represents status of L929 cells viability upon the treatment with TNF+CHX and TNF+ zVAD for 4 and 11 hours, which has been plotted based on the data obtained from Flow Cytometry. X-axis indicates selectively chosen control groups of the most importance: untreated L929 cells stated as "UT"; experimental control of L929 cells treated with TNF+CHX; and experimental control of L929 cells treated with TNF+zVAD. Y-axis represents % of cell death

5.2 Cells dying by necroptosis contributes to maturation of DCs *in vitro*

Due to the fact that significant number of cells die during the time required to generate immature dendritic cells from monocytes, we decided to add 10 μ M zVAD-fmk to the cell medium on day three, five and six of incubation time and leave the cells until they will be harvested (on day seven) (see Appendix 4). We did it, in order to block caspases activity and thus to “switch” the cell death from apoptotic to necroptotic. For all conditions, culture time was exactly the same i.e. all cells were harvested on day seven and maturation status of DCs was determined based on the level of expression of DCs surface markers: CD83, CD86 and HLA-DR detected by Flow Cytometry. In Figure 10 we can see that addition of zVAD on day three contributed to the highest expression of cell surface markers.

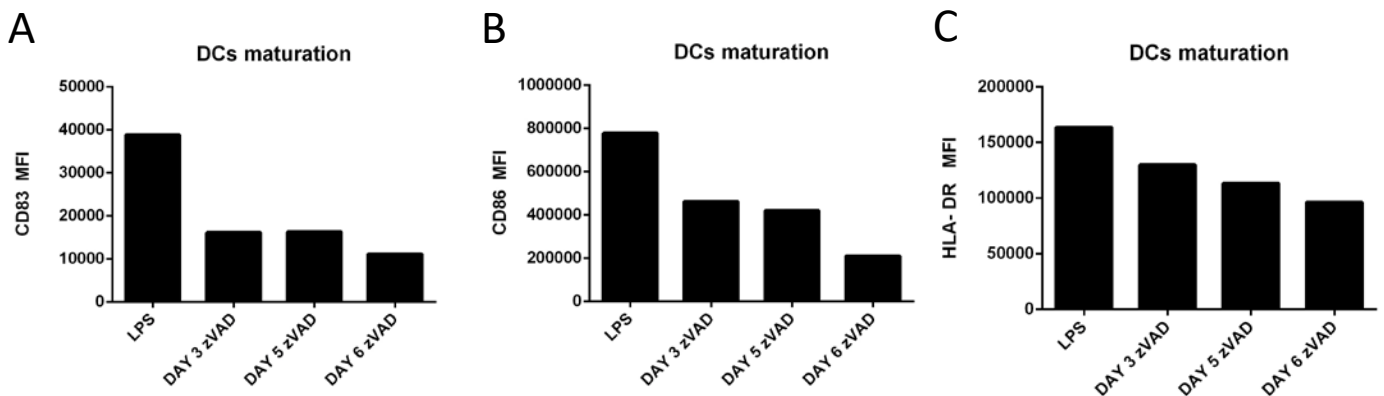


Figure 10 Evaluation of dendritic cells maturation status, upon addition of 10 μ M zVAD-fmk to the cell culture on day three, five and six of DCs generation process. DCs maturation has been estimated based on the expression level of cell surface markers: HLA-DR (A), CD86 (B) and CD83 (C), which are up-regulated when DCs are activated. X-axis represents controls: a positive control of LPS-matured moDCs added on day six; and the experimental groups, in which moDCs were treated with 10 μ M zVAD-fmk either on day three, five or six. Y-axis shows median fluorescence intensity (MFI) of the surface marker.

5.3 Supernatant collected from dead L929 cells mature DCs

Necroptotic cells might release damage-associated molecular patterns (DAMPs) to the extracellular space, and thereby potentially mature dendritic cells. In order to test if apoptotic or necroptotic cells could induce maturation of moDCs, cell death in L929 cells was induced upon the treatment with TNF/CHX or TNF/zVAD for 11 hours. Then, the supernatant collected from dead L929 cells have been added to immature DCs on day six as a “maturation stimuli” (Appendix 3). Status of DCs was determined based on the level of expression of DCs surface markers: CD83, CD86 and HLA-DR detected by Flow Cytometry. In Figure 8 we can see that supernatant from TNF/zVAD-treated L929 cells resulted in the highest maturation level of DCs.

DCs maturation status after exposure to 100 μ l supernatant, collected from dead L929 cells treated for 11hrs

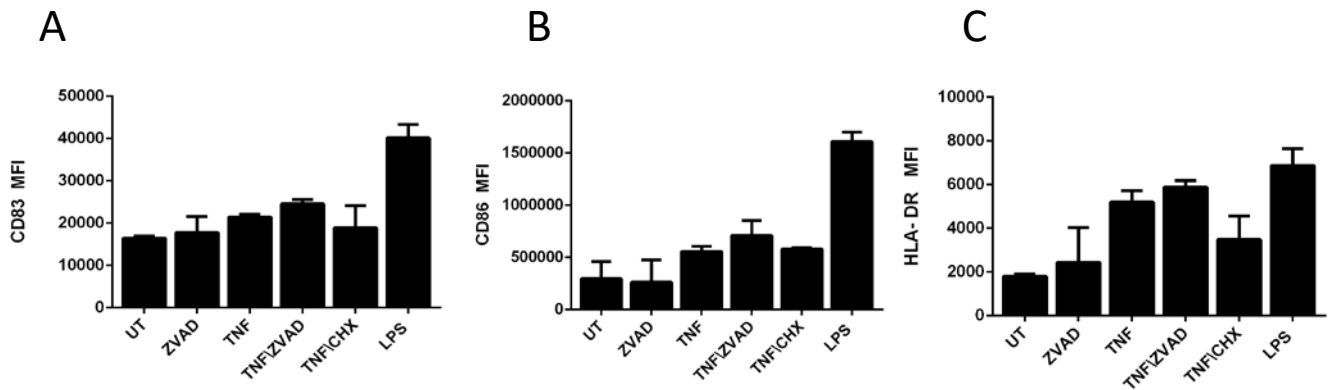


Figure 11 Evaluation of dendritic cells maturation status, upon exposure to 100 μ l supernatant collected from dead L929 cells. DCs maturation has been estimated based on the expression level of cell surface markers: HLA-DR (A), CD86 (B) and CD83 (C), which are up-regulated when DCs are activated. X-axis represents treatment of L929 cells, from which 100 μ l supernatant have been collected and added to immature moDCs as a “maturation stimuli” on day six of moDCs generation process. Each column represents mean value of median fluorescence intensity (MFI) collected from 2 replicates. Error bars indicate standard deviation between 2 replicates.

Titration experiment was performed to evaluate if and at which concentration cGAMP can induce maturation of moDCs.

Four different concentrations of cGAMP (0.2 μ M, 2 μ M, 20 μ M, 100 μ M) were added either on day tree or day six to the moDCs cell culture. Below, selectively chosen histograms represent the maturation status of moDCs exposed to the lowest (0.2 μ l cGAMP) and highest (100 μ l cGAMP) concentrations only on day 6. For the full overview of four different concentrations of cGAMP (0.2 μ M, 2 μ M, 20 μ M, 100 μ M) and comparison between stimulation on day tree and six, see Appendix 5-12.

From the Figures 12-14 we can observe significant difference at the expression levels of all DCs surface markers upon the treatment with the highest concentration of cGAMP ,as compared to the lowest concentration used.

DAY 6 CD83 SURFACE MARKER EXPRESSION

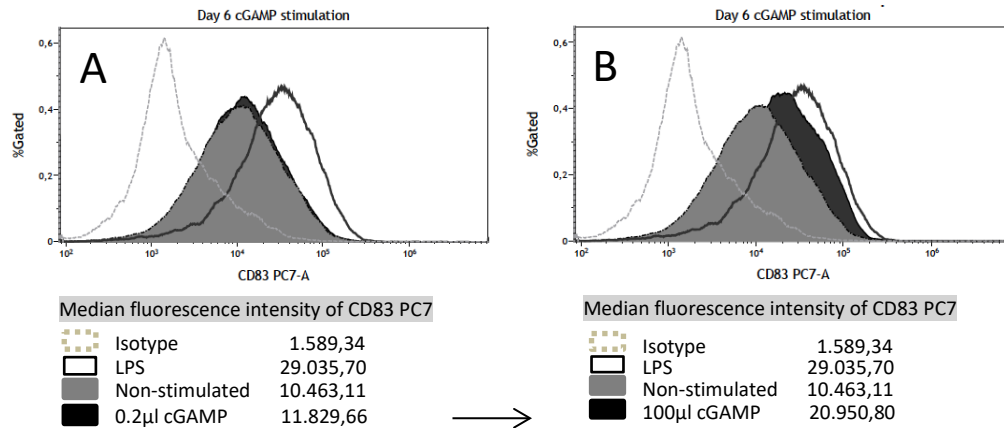


Figure 12 Histograms A & B represent changes of CD83 surface marker expression: A- 0.2µl cGAMP, the lowest concentration added on day 6 of incubation time; B- 100µl cGAMP, the highest concentration added on day 6 of incubation time. The x-axis shows the fluorescence intensity of CD83-PC7, and additionally, median fluorescence intensity of CD83 PC7 from each of the curve is shown in the form of numbers. The y-axis shows the percentage of cells in the gate. In each histogram there are four curves; an isotype control (grey dotted line), a non-stimulated moDCs (curve filled with grey colour), a positive control- the sample stimulated with LPS (100 ng/ml) (thick black line), and moDCs exposed to cGAMP (curve filled with black colour).

DAY 6 CD86 SURFACE MARKER EXPRESSION

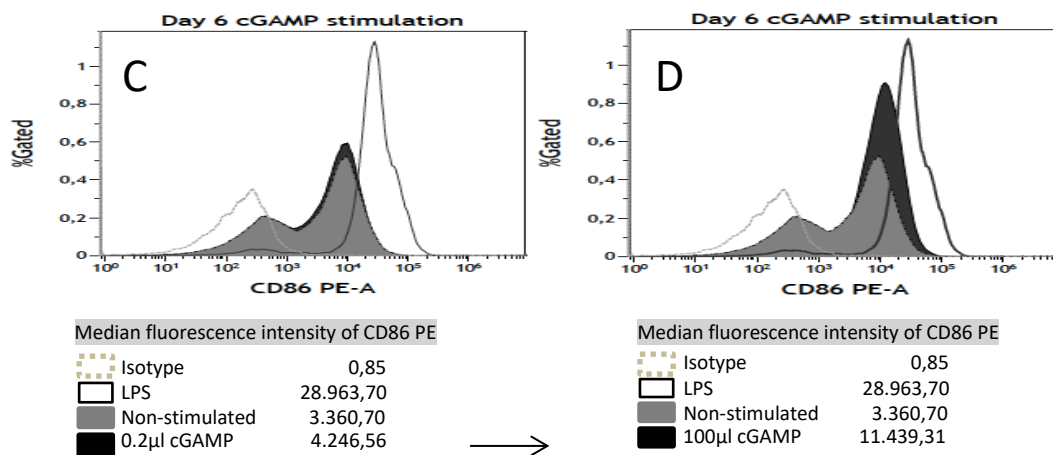


Figure 13 Histograms C & D represent CD86 surface marker expression: A- 0.2µl cGAMP, the lowest concentration added on day 6 of incubation time; B- 100µl cGAMP, the highest concentration added on day 6 of incubation time. The x-axis shows the fluorescence intensity of CD86-PE, and additionally, median fluorescence intensity of CD86 PE from each of the curve is shown in the form of numbers. The y-axis shows the percentage of cells in the gate. In each histogram there are four curves; an isotype control (grey dotted line), a non-stimulated moDCs (curve filled with grey colour), a positive control- the sample stimulated with LPS (100 ng/ml) (thick black line), and moDCs exposed to cGAMP (curve filled with black colour).

Day 6 HLA-DR SURFACE MARKER EXPRESSION

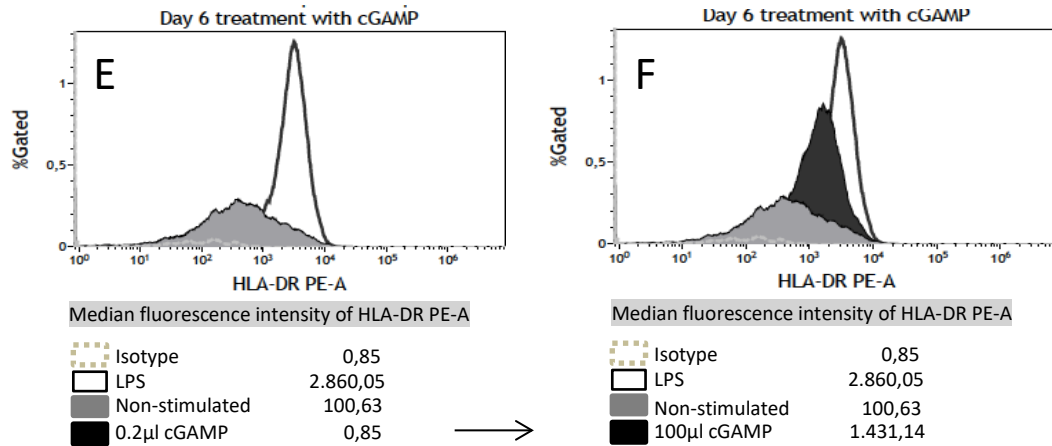


Figure 14 Histograms E & F represent HLA-DR surface marker expression: A- 0.2μl cGAMP, the lowest concentration added on day 6 of incubation time; B- 100μl cGAMP, the highest concentration added on day 6 of incubation time. The x-axis shows the fluorescence intensity of HLA-DR PE-A, and additionally, median fluorescence intensity of HLA-DR PE-A from each of the curve is shown in the form of numbers. The y-axis shows the percentage of cells in the gate. In each histogram there are four curves; an isotype control (grey dotted line), a non-stimulated moDCs (curve filled with grey colour), a positive control- the sample stimulated with LPS (100 ng/ml) (thick black line), and moDCs exposed to cGAMP (curve filled with black colour).

For a better overview of the level of DCs maturation, a bar chart of median fluorescence intensity (MFI) was created for three cell surface markers: CD83, CD86 and HLA-DR using Prism 6 program (Figure 15).

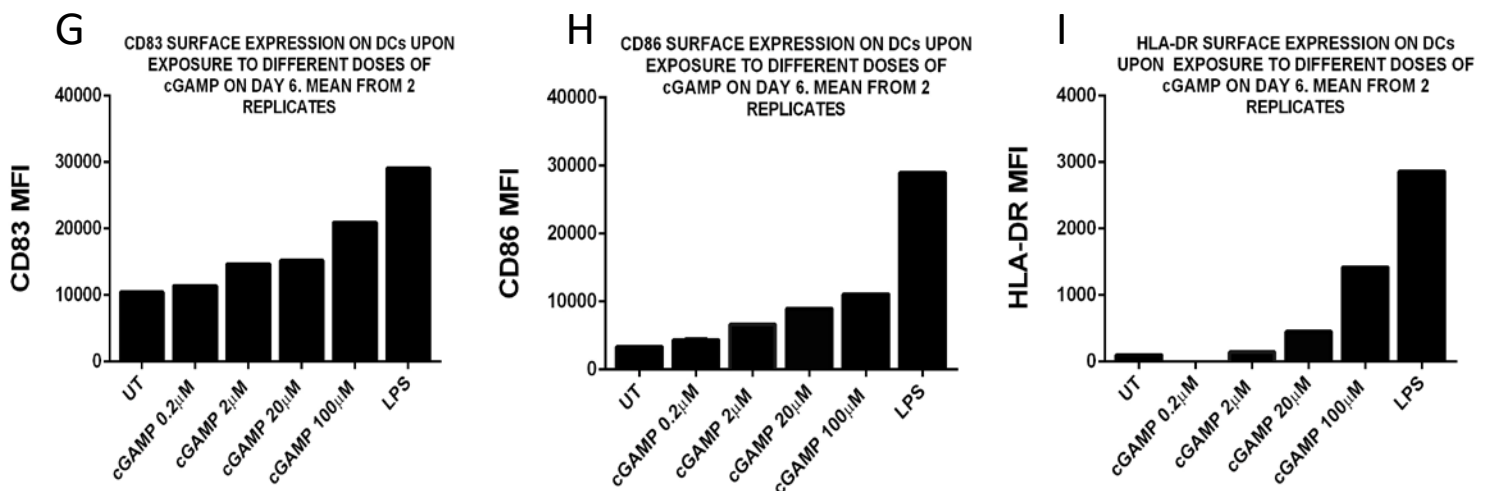


Figure 15 Summary of cGAMP titration experiment. Evaluation of dendritic cells maturation status, upon treatment with different cGAMP doses added on day six have been estimated based on the expression level of cell surface markers: CD83 (G), CD86 (H), and HLA-DR (I), which are up-regulated when DCs are activated. In each bar chart, the Median Fluorescent Intensity (MFI) of the individual surface marker represents the mean value obtained from 2 replicates.

5.5 cGAMP matures Dendritic Cells more potent than ATP and Uric Acid Crystals.

In order to evaluate how strong is the effect of cGAMP on moDCs maturation in comparison to known DAMPs: ATP and Uric Acid crystals, I treated moDCs on day six with the equivalent molar concentration of these molecules. In Figure 16 it can be observed that treatment with cGAMP contributed to moDCs activation much better than ATP or UAC.

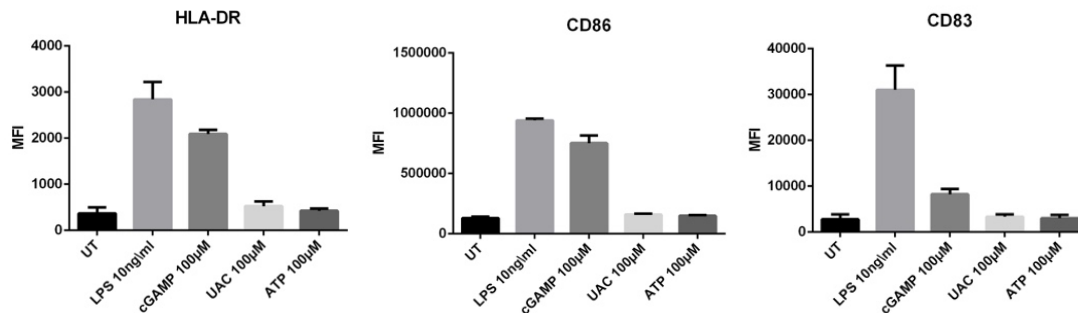


Figure 16 Evaluation of dendritic cells maturation status, upon treatment with equivalent molecular concentration of cGAMP, Uric Acid and ATP. DCs maturation has been estimated based on the expression level of cell surface markers: HLA-DR (A), CD86 (B) and CD83 (C), which are up-regulated when DCs are activated. X-axis represents controls: a negative control stated as “UT” indicates untreated moDCs; a positive control of LPS-matured moDCs; and the experimental groups, in which moDCs were treated with either cGAMP, Uric Acid stated as “UAC” or ATP. Each column represents mean value of median fluorescence intensity (MFI) collected from 2 replicates. Error bars indicate standard deviation between 2 replicates.

5.6 Co-culture of T cells with cGAMP-matured DCs resulted in T cells proliferation and increased levels of the cytokines: IL-10, IL-1 β and INF γ detected by multiplex assay MSD.

Dendritic cells respond towards environmental factors by regulating the adaptive immune system through activation and priming of T cells. Mixed leukocytes reaction (MLR) was performed in order to determine the cytokine profile secreted by immune cells upon co-culture of cGAMP-matured DCs with T cells. The cytokines in each sample were determined and quantified using MSD Human TH1/TH2 10-Plex Assay and the results are shown in the form of bar charts below. Moreover, PBMCs from donor 2 were stained with eFluor 670 prior the MLR and the proliferation status was detected by flow cytometry (Figure 17 A). It should be noted that “T cells proliferation” refers to PBMCs proliferation. The gating method is shown in Appendix 13.

Four days co-culture of cGAMP-treated moDCs with PBMCs, resulted in higher % of PBMCs proliferation, as compared to the effect of moDCs treated with LPS. The cytokine profile revealed elevated levels of IL-10, IL-1 β and IFN- γ upon co-culture of cGAMP-treated moDCs with PBMCs (Figure 17 B,C).

APCs cytokines

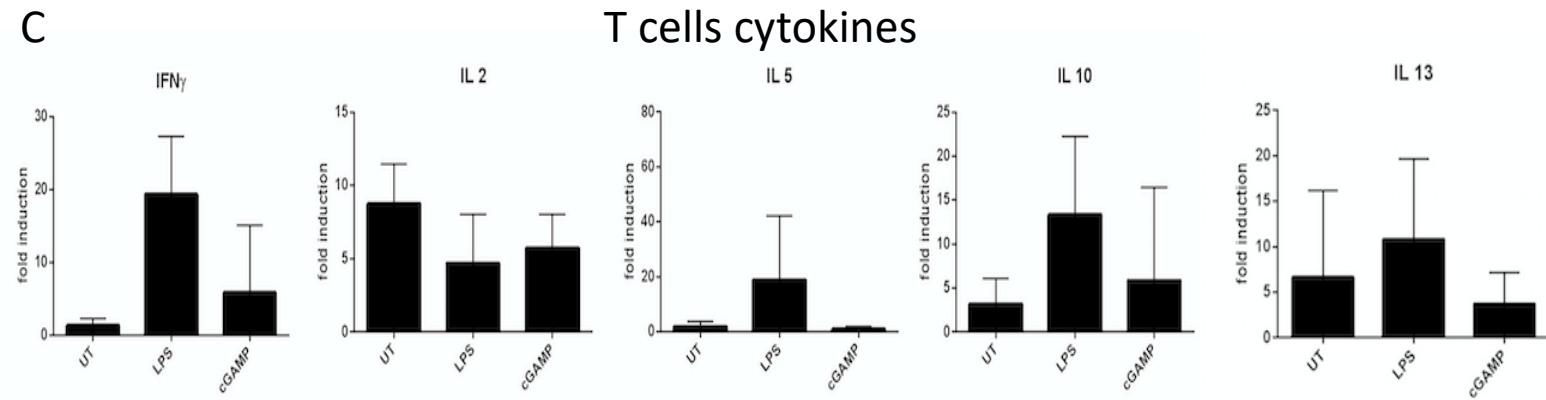
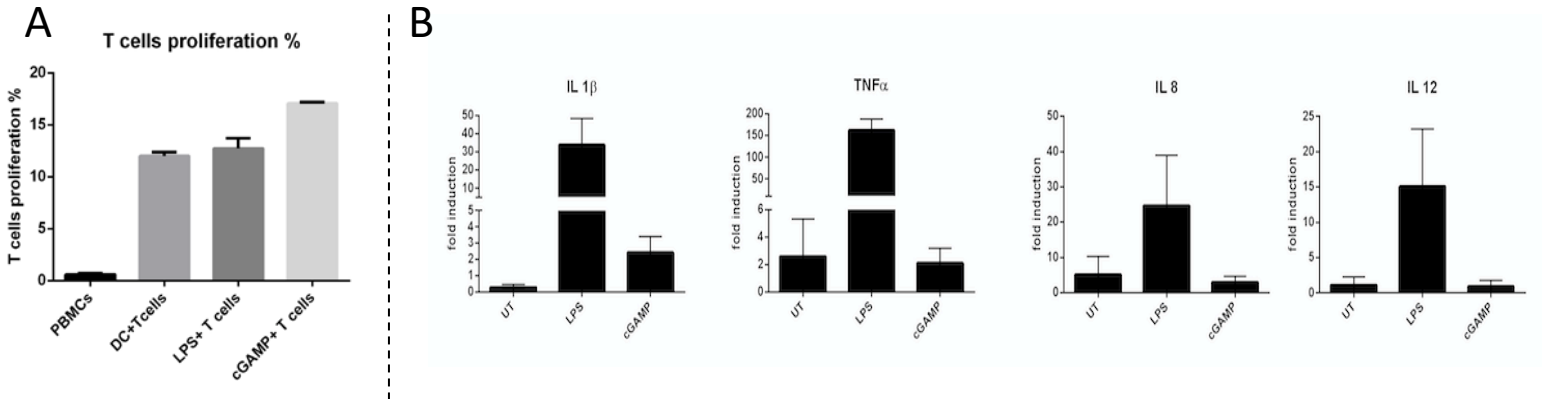


Figure 17 A) The effect on immune cells proliferation upon co-culture of stained with eFluor 670 PBMCs with cGAMP-treated moDCs. X-axis represents controls: PBMCs stained with eFluor 670 only; a control of untreated moDCs co-cultured with PBMCs, stated as “DC+ T cells”; a control of LPS-treated moDCs co-cultured with PBMCs, stated as “LPS+ T cells”; and cGAMP-treated moDCs co-cultured with PBMCs stated as “cGAMP+T cells”. Revealed cytokines profile from the mixed leukocyte reaction (MLR) experiment; determined and quantified using Meso Scale Discovery multiplex assay (MSD). Cytokines profiles have been divided into 2 groups: “APCs cytokines” and “T cells cytokines” which have been grouped based on the type of immune cells, which are known to produce them. X-axis represents controls: a negative control stated as “UT” representing untreated moDCs co-cultured with T cells; a positive control “LPS”, which represents co-culture of LPS-matured moDCs with T cells; and an experimental group stated as “cGAMP” that represents co-culture of cGAMP-matured DCs with T cells. The fold induction value on Y-axis is relative to the value detected in the control of untreated DCs that were not co-cultured with T cells. MSD have been performed three times and error bars represent standard deviation between replicates.

6. Discussion

Tumour necrosis factor alfa (TNF α) upon binding to tumour factor receptor 1 (TNFR1) can activate both transcription factors, such as promoting cell survival NF- κ B, as well as cell death mechanisms (Figure 4). Most cell lines are not killed by the addition of TNF α alone, but many die when TNF α is added together with inhibitors of transcription or translation factors, such as cycloheximide (CHX), which inhibits NF- κ B pro-survival pathway and thus activates programmed cell death- apoptosis. Depending on the cell type and circumstances, TNF α in the presence of pancaspase inhibitory compound- zVAD-fmk switches the mode of cell death from apoptosis to programmed necrosis, termed necroptosis (Moujalled *et al.*, 2013).

Initially, I set out to choose a cancer line, in which the cell death can be induced upon the treatment with apoptotic TNF α plus CHX or necroptotic TNF plus zVAD-fmk conditions. The crucial criterium for choosing relevant cell lines was the expression of RIPK3, which is essential for TNF α -induced necroptosis. Recent studies show that RIP3 expression is often silenced in cancer cells due to genomic methylation near its transcriptional start site, thus activation of necroptosis in those cells is largely repressed. Based on the studies conducted by (He *et al.*, 2009; Koo *et al.*, 2015; Moriwaki *et al.*, 2015), which revealed several cancer cell lines expressing RIPK3, I have chosen to take under the investigation two of them: the murine fibrosarcoma cell line L929 and the human colon adenocarcinoma cell line HT-29, which are commonly used cell lines in cell death induction experiments *in vitro*. Upon the treatment with combination of TNF+CHX or TNF+ zVAD, cell death was observed only in L929 cells (Figure 9), whereas high cells viability was maintained in HT-29 cells even up to 103hrs incubation time (Appendix 1). One of the explanations may be the fact that we do not know the origin of HT-29 cells as the cell line was a gift. Therefore, the numerous passage experience could have affected the cellular physiology and thus the response to the stimuli. Based on these results, I decided to choose L929 cells as a model for the cell death induction in this study.

The next step was to investigate the effect of necroptotic cells on DCs maturation status. In order to block caspases activity in the cell death signalling pathway, zVAD-fmk was added to DCs culture medium on day three, five and six of monocyte-derived DCs generation process. By the time monocytes will differentiate into immature DCs (over the seven days incubation time), up to 50% of seeded primary cells will die. It should be noted, that the addition of zVAD-fmk on day three could contribute to activation of M1 type macrophages rather than DCs, as CD86 surface marker is characteristic for both cell types (Zarif *et al.*, 2016). Nonetheless, addition of zVAD-fmk on day five resulted in higher expression of all DCs maturation markers compared to moDCs exposed to zVAD on day six. Therefore, it may be concluded that necroptotic cells did contribute to maturation of moDCs. These results can be supported with the study performed by (Aaes *et al.*, 2016), where they show that co-culture of necroptotic cancerous CT26 cells with primary bone marrow derived dendritic cells (BMDCs) highly induce DCs maturation *in vitro*. Additionally, they show that neither BMDCs co-cultured with accidental necrotic cells nor BMDCs co-cultured with live cancer cells did alter DCs

maturation, indicating that only cells undergoing programmed necrosis contribute to DCs maturation.

Furthermore, in order to evaluate the effect of necroptotic cancer cells on the adaptive immune system *in vivo*, they vaccinated BALB/c mice with necroptotic CT26 cells. They could observe that immunization prevented tumour growth at the challenge site. Moreover, in the isolated lymph nodes from immunized mice, they identified the presence of tumour antigen-specific cytotoxic CD8a⁺ T cells, thus validating the ability of necroptotic cells to induce a potent immune response in *in vivo* system.

In another study, performed by (Woo *et al.*, 2014), it was indicated that STING pathway is required for spontaneous cytotoxic CD8a⁺ T cells responses against tumour derived-antigens. They also showed that CD8a⁺ T cells priming was attenuated in STING-deficient mice and thus confirming the importance of STING activation pathway in anti-tumour immunity. Furthermore, they demonstrated that tumour-derived DNA was transferred to host antigen presenting cells (APCs) present within the tumour microenvironment (TME), and by tracking tumour-labelled DNA, they localized it in the cytosol of APCs. Due to the fact that the presence of tumour DNA in the cytoplasm provides an easy access to the activation of STING, they observed resulting production of IFN β by APCs via a STING-dependent fashion.

The question arise what makes necroptotic cells immunogenic and how they contribute to STING activation?

It has been suggested that endogenous adjuvants released from dying cells are capable of initiating immune cells activation.

Several studies revealed that chemotherapy and radiotherapy lead to release of ATP and HMGB1 from treated cancer cells and these molecules contributed to DCs activation, which in turn resulted in priming of antitumor T cells (Apetoh *et al.*, 2007; Deng *et al.*, 2014). On top of that, in the study conducted by (Ahn *et al.*, 2014), they showed that etoposide-a commonly used drug in chemotherapy - caused DNA damage of tumour cells and lead to nucleosome leakage into the cytosol, which resulted in STING-dependent cytokine production of type I IFNs. It is known that upon recognition of damaged DNA fragments in the cytosol, cGAS synthesize a small second messenger molecule cGAMP (675Da), which binds directly to STING receptor and induce the production of type I IFNs, mainly IFN α and IFN β (Li *et al.*, 2016). All of the studies mentioned so far, linked the recognition of DNA as the key activator of cGAS-STING pathway. It could be speculated that, once the cell membrane is ruptured (like in the case of necroptosis), cGAMP may be released to extracellular environment and hence in turn activates the immune system. It has also been shown that necroptotic material is coingested with the extracellular fluid by antigen-presenting cells (APCs) via micropinocytosis (Krysko *et al.*, 2006). Thus, it could explain the way, in which molecules from the medium are engulfed by DCs.

Recently more studies have investigated the effect of cGAMP on the adaptive immune response suggesting the use of cGAMP as STING agonist in strategies to improve cancer therapies. In the study conducted by (Deng *et al.*, 2014) they demonstrated that intertumoral administration of cGAMP in mice right after radiation, effectively reduced tumour burden, as compared to the effect of radiation alone.

We hypothesised that cGAMP could be one of the damage associated molecular patterns (DAMPs) released from necroptotic cells. To evaluate that, we treated moDCs with supernatant collected from either TNF/CHX- treated L929 cells or TNF/ zVAD- treated L929 cells. In Figure 11 it can be observed that supernatant obtained from TNF/ zVAD- treated L929 cells contributed to the highest expression of DCs maturation markers. Yet, it should be acknowledged that TNF α itself can mature DCs (Ebrahimi *et al.*, 2009). Therefore, it is difficult to interpret, whether TNF α administered directly to the medium, which then was collected and added as a “stimuli” to moDCs, matured them itself, or rather endogenous substances from necroptotic cells, which could contribute to DCs activation. On the other hand, in the past papers, it has been claimed that treatment with TNF α alone was sufficient to trigger programmed necrosis, exclusively in L929 cells (Vercammen *et al.*, 1998; Vanlangenakker *et al.*, 2011; Maeda and Fadeel, 2014). If that is true then we may interpret, as released molecules from TNF α plus zVAD-treated L929 cells could contribute to moDCs maturation. Nonetheless, whether or not DCs maturation was triggered by released molecules from dead cells or just by the TNF α presence from the medium, is hard to be concluded based on these data. Therefore, we have performed additional experiment, in which we have indicated that administration of lower TNF α concentrations 0.75; ng/ml was enough to kill L929 cells with combination of zVAD-fmk (Appendix 14) . Hence, we conclude that released endogenous substances from necroptotic cells could result in DCs activation. Further, we decided to evaluate whether cGAMP itself matures moDCs *in vitro*. To do that, titration experiment was performed to determine which concentration of cGAMP is sufficient to trigger maturation of moDCs. From the results in Figures 14-15, we observed that treatment with the highest concentration applied: 100 μ M cGAMP induced the strongest maturation of moDCs. These results, demonstrating ability of cGAMP to mature DCs, are in line with other studies conducted by: (i) (Škrnjug, Guzmán and Ruecker, 2014), where they showed that cGAMP directly activated murine and human DCs *in vitro* and (ii) (Li *et al.*, 2016), where they show DCs activation *in vivo*, upon the injection of tumour-bearing mice with cGAMP.

Further we showed that cGAMP resulted in stronger up-regulation of maturation markers than treatment with equivalent molar concentration of ATP or Uric Acid Crystals (UAC). Cytokine secretion by dying tumour cells has been shown to enhance the anti-tumour immunity. Upon co-culture of PBMCs with cGAMP-matured DCs, we have revealed the increased production of cytokines: IL-10, IL-1 β and IFN γ . Consistent with the study of (Li *et al.*, 2016) we detected increased IFN γ production upon the treatment with cGAMP.

7. Conclusion

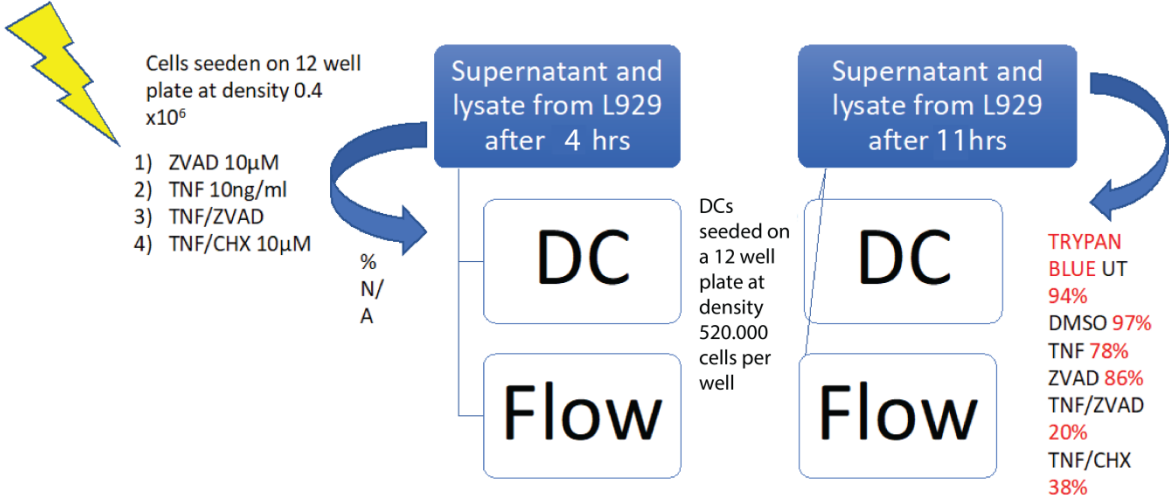
Based on our results, showing that dead L929 cells, as well as supernatant collected from dead L929 cells, contributed to maturation of moDCs, we can speculate that cGAMP could be one of the DAMPs released by necroptotic cells.

8. Future prospects

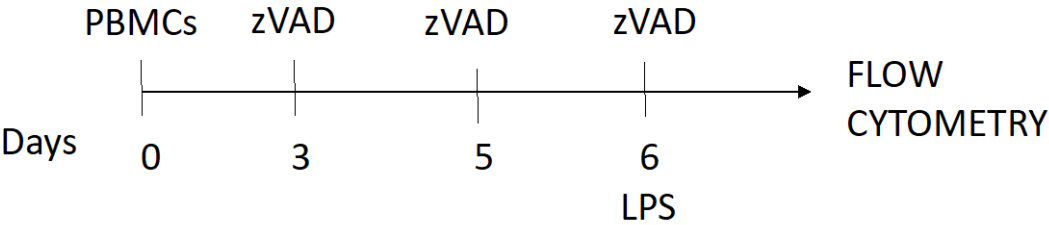
In order to induce necroptosis in HT-29 cells, addition of zVAD-fmk in combination with TNF+CHX or TNF+ SMAC mimetic is required, as stated in studies of (He *et al.*, 2009; Koo *et al.*, 2015).

Further analysis need to be done in order to confirm whether treated L929 cells undergoes apoptosis or necroptosis. The importance of this is to prove that cGAMP together with other DAMPs is released from necroptotic cells, as a result of membrane rupture. PARP is the first protein known to be cleaved by caspases activation, a feature characteristic for apoptotic cell death mode. It should be able to detect the cleavage of PARP by Western Blot. Although, I tried several times to identify the PARP cleavage in the cell lysates obtained from dead cells, the amount of proteins (as detected by Pierce BCA Protein Assay) was too low to be visualised on the nitrocellulose membrane. The lack of proteins was also confirmed by staining the membrane with an organic dye Ponceau S. In the future trial, it might be possible that higher number of cells should be taken into consideration. Moreover, flow cytometry using Annexin V/ propidium iodine (PI) assay could be performed to distinguish apoptotic cells from necroptotic cell death. Furthermore, mass spectrometry analysis of the lysate collected from dead cells could determine the possible presence of cGAMP released from necroptotic cells. It would be also interesting to evaluate where cGAMP accumulation is higher in the cytoplasm of dead cell or nucleus and hence to determine the movement of cGAMP during necroptosis.

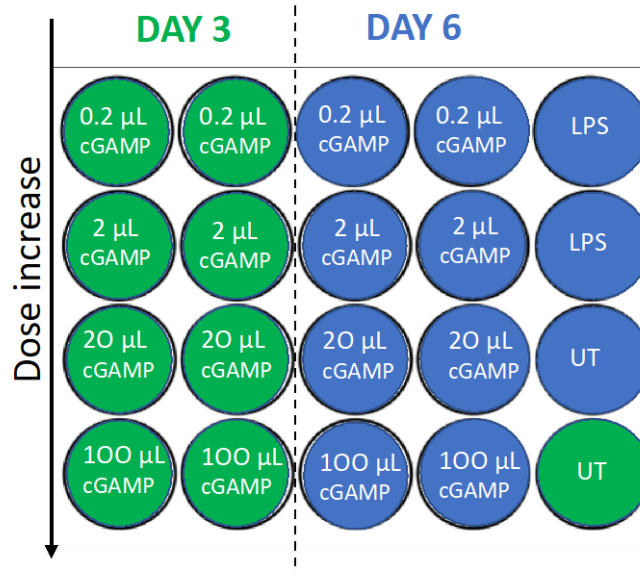
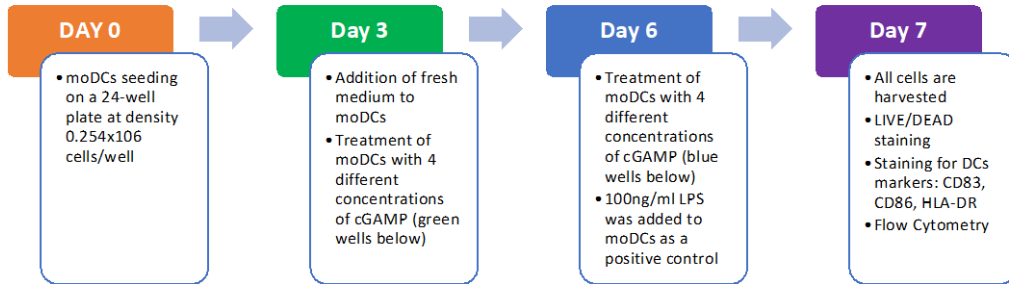
APPENDIX 3. TREATMENT OF moDCs WITH SUPERNATANT OBTAINED FROM DEAD L929 CELLS.



APPENDIX 4. ADDITION OF Z-VAD TO DC'S DURING GENERATION PROCE



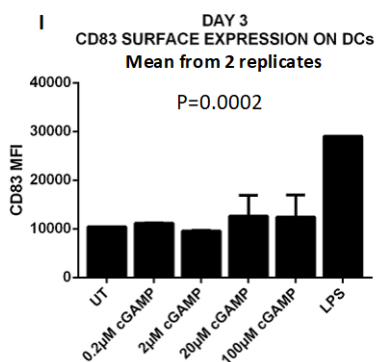
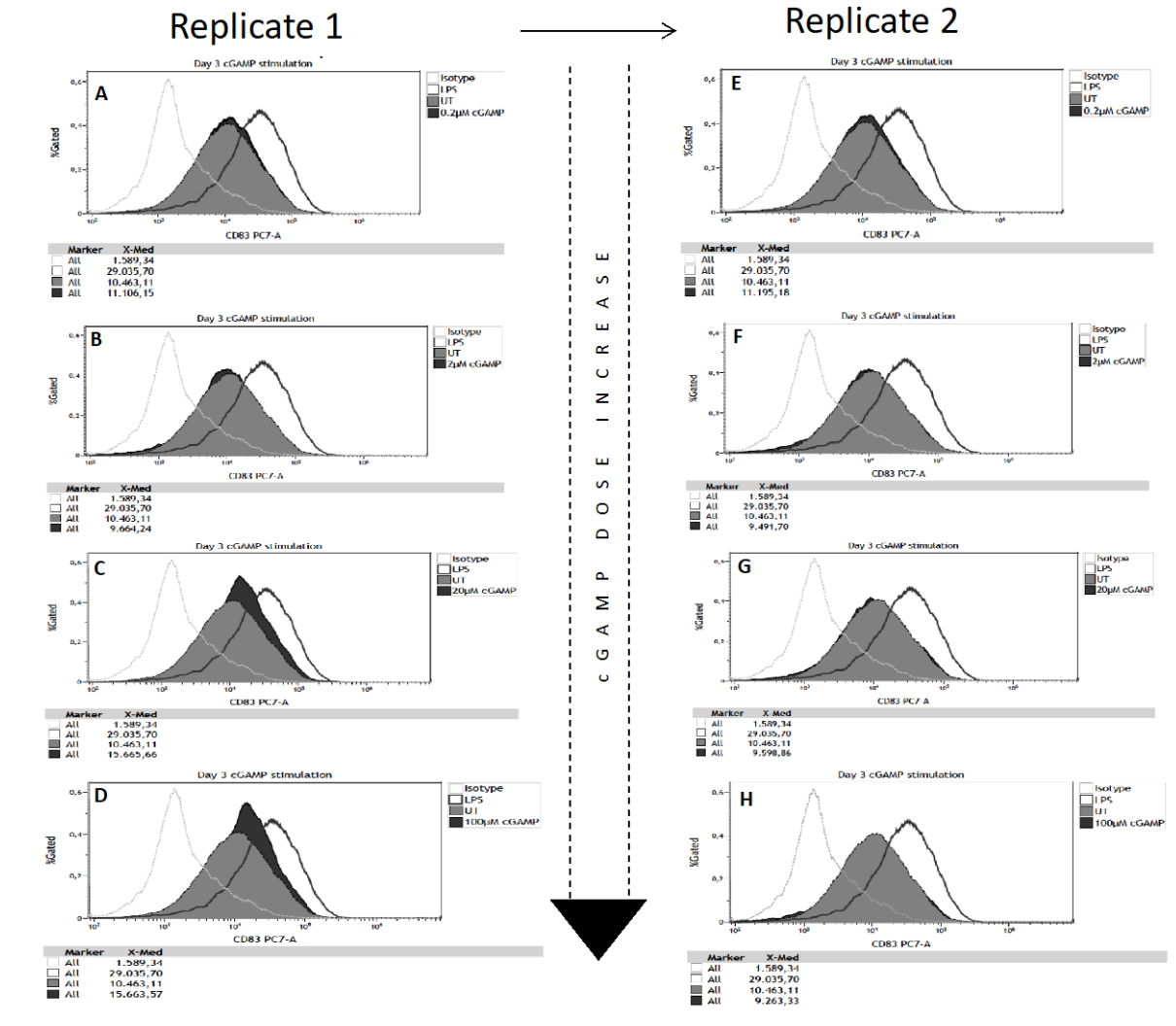
APPENDIX 5. cGAMP TITRATION EXPERIMENT. ESTIMATING OPTIMAL cGAMP CONCENTRATION, WHICH TRIGGERS DCs MATURATION.



On Day 0, moDCs were seeded on a 24-well plate at density 0.254×10^6 cells per well and were cultured in fully supplemented medium as described in methods section. Four different concentrations of cGAMP (0.2 μ M, 2 μ M, 20 μ M, 100 μ M) were added either on day tree (green wells) or day six (blue wells) to the cell culture. Each concentration was added in 2 replicates. On Day 6, 100ng/ml LPS was added to moDCs as a positive control (blue wells). All cell were cultured until day 7, when they were harvested, stained, and analysed by Flow Cytometry (see timeline above).

APPENDIX 6. DAY 3 CD83 SURFACE MARKER

CD83 marker expression. DCs were exposed to different concentration of cGAMP on day 3 of incubation time. Each concentration was added in 2 replicates.

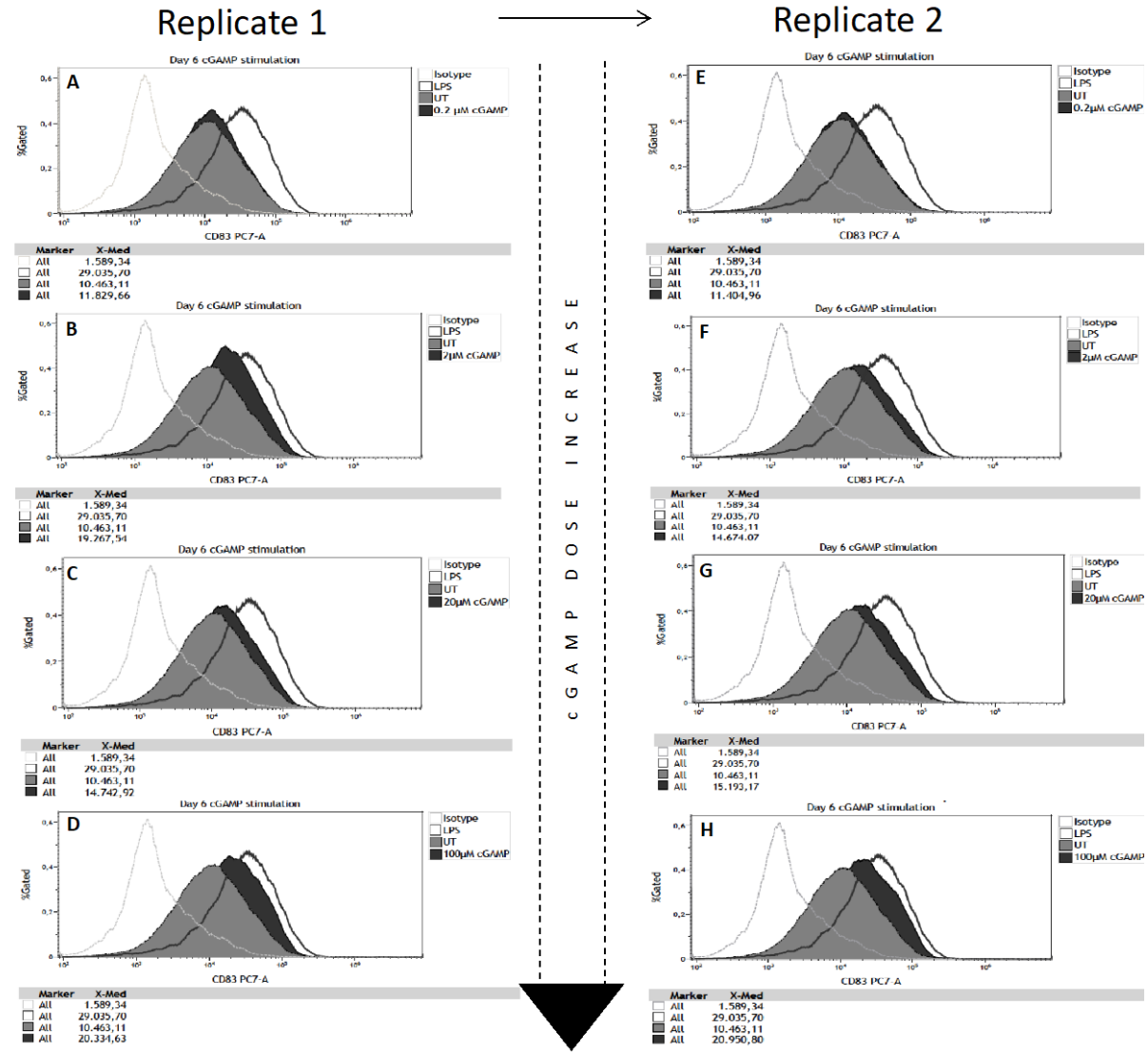


Histograms represent CD83 surface marker expression. In each histogram there are four curves; an isotype control (grey dotted line), a non-stimulated moDCs -stated as UT (curve filled with grey colour), a positive control- the sample stimulated with LPS (100 ng/ml) (thick black line), and moDCs exposed to cGAMP (curve filled with black colour). The x-axis shows the fluorescence intensity of CD83-PC7, and additionally, median fluorescence intensity of CD83 PC7 from each of the curve is shown in the form of numbers, stated as "X-med". The y-axis shows the percentage of cells in the gate. A-D represent data from replicate 1, from the lowest 0.2µl cGAMP concentration to the highest 100µl cGAMP; same for replicate 2 (E-H).

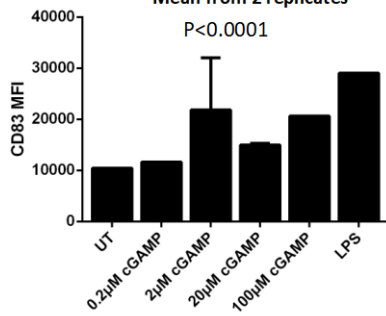
For a better overview, data from histograms is plotted in the form of bar chart (I). Each column represents mean value of CD83 MFI collected from 2 replicates. Error bars indicate standard deviation between 2 replicates. P value was generated with ordinary one-way ANOVA test in Prism 6 program.

APPENDIX 7. DAY 6 CD83 SURFACE MARKER

CD83 marker expression. DCs were exposed to different concentration of cGAMP on day 6 of incubation time. Each concentration was added in 2 replicates.



I DAY 6 CD83 SURFACE EXPRESSION ON DCs
Mean from 2 replicates

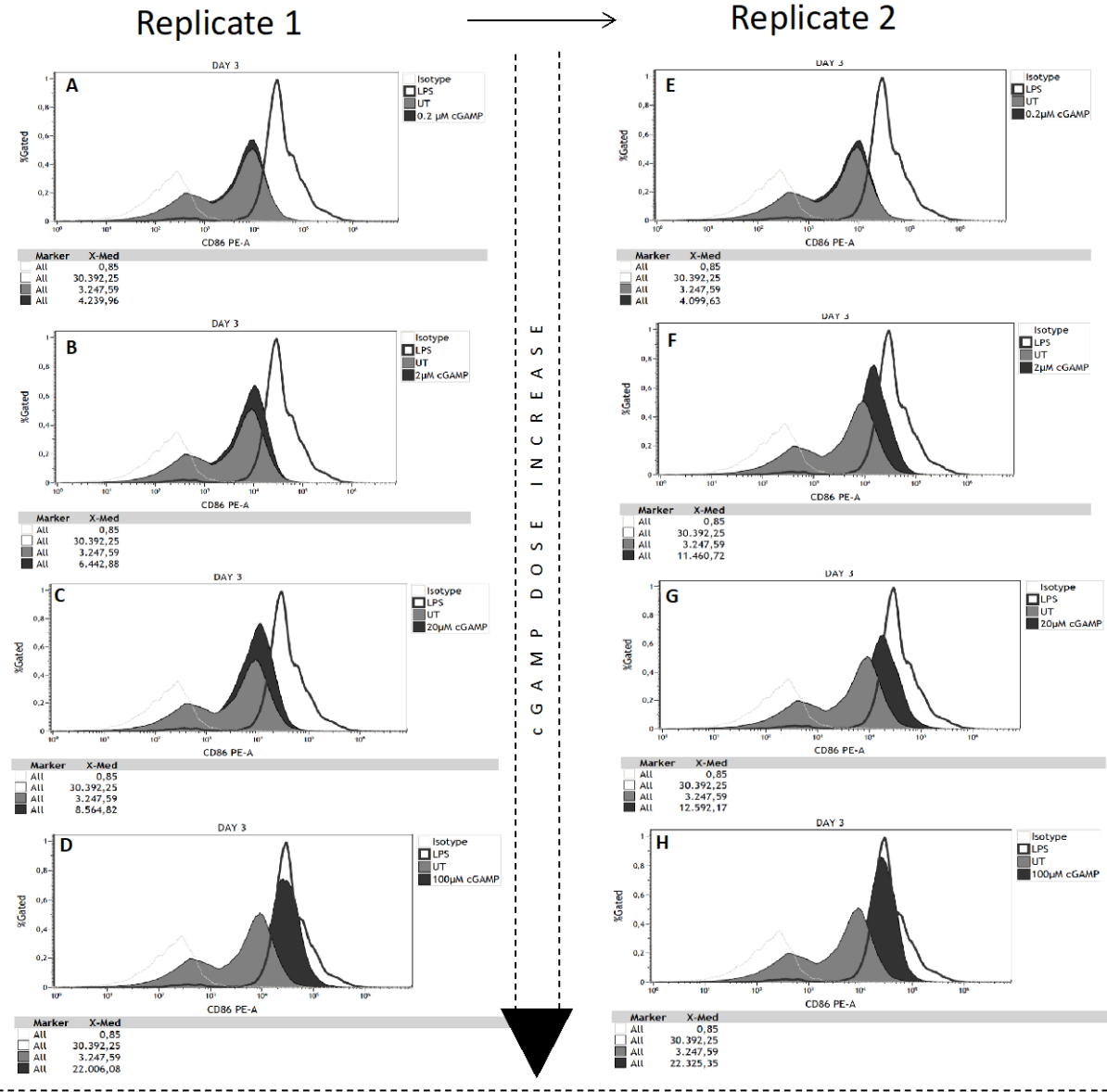


Histograms represent CD83 surface marker expression. In each histogram there are four curves; an isotype control (grey dotted line), a non-stimulated moDCs - stated as UT (curve filled with grey colour), a positive control- the sample stimulated with LPS (100 ng/ml) (thick black line), and moDCs exposed to cGAMP (curve filled with black colour). The x-axis shows the fluorescence intensity of CD83-PC7, and additionally, median fluorescence intensity of CD83-PC7 from each of the curve is shown in the form of numbers, stated as "X-med". The y-axis shows the percentage of cells in the gate. A-D represent data from replicate 1, from the lowest 0.2µl cGAMP concentration to the highest 100µl cGAMP; same for replicate 2 (E-H).

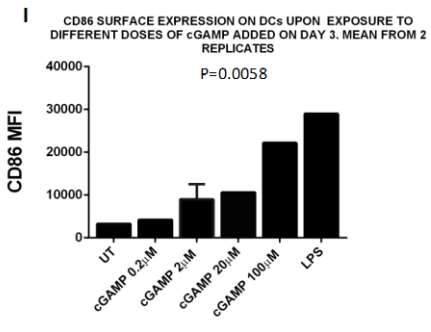
For a better overview, data from histograms is plotted in the form of bar chart (I). Each column represents mean value of CD83 MFI collected from 2 replicates. Error bars indicate standard deviation between 2 replicates. P value was generated with ordinary one-way ANOVA test in Prism 6 program.

APPENDIX 8. DAY 3 CD86 SURFACE MARKER

CD86 marker expression. DCs were exposed to different concentration of cGAMP on day 3 of incubation time. Each concentration was added in 2 replicates.



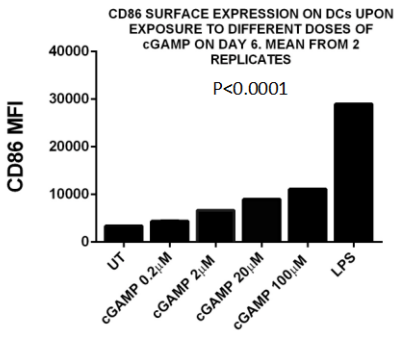
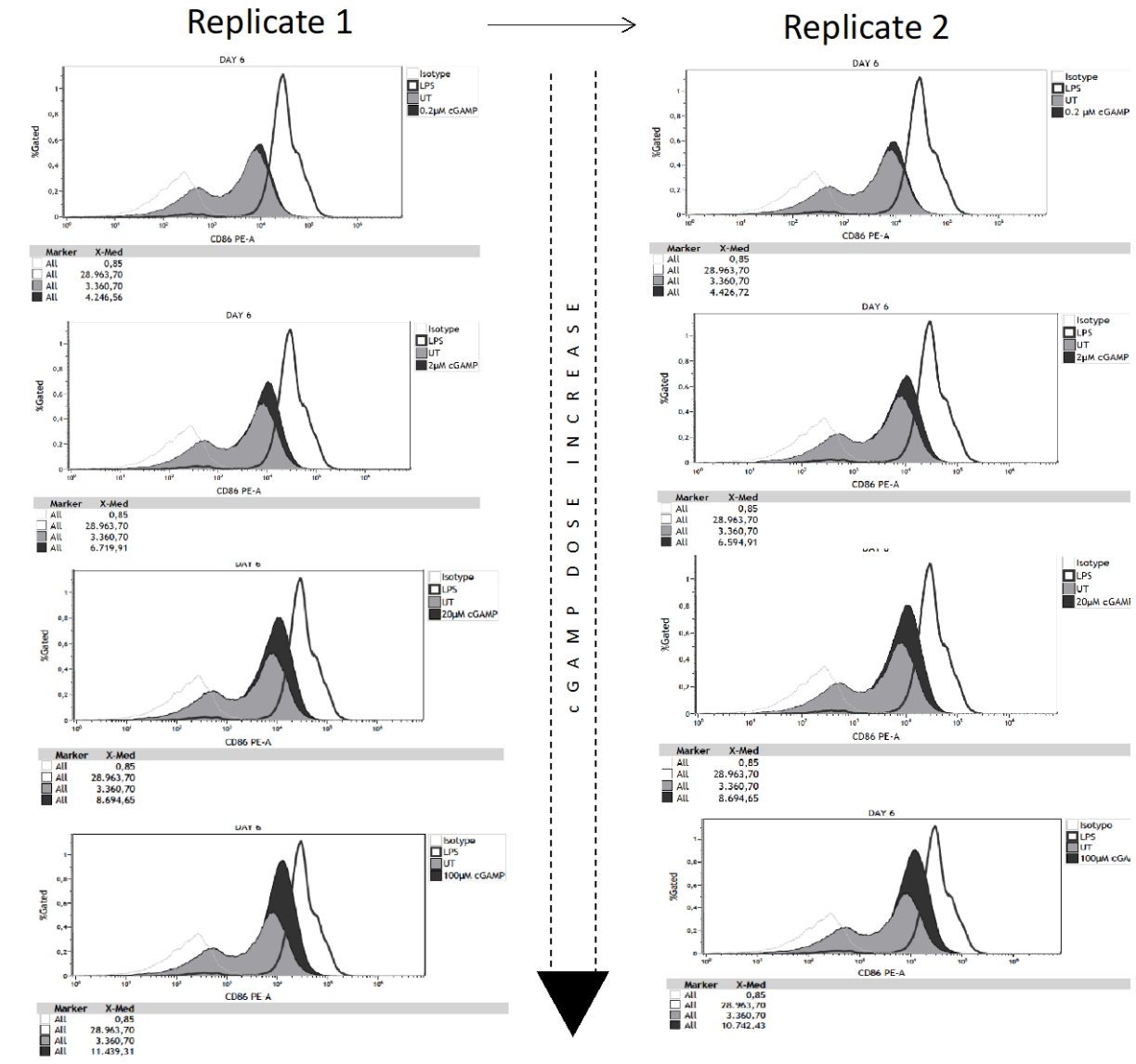
C G A M P D O S E I N C R E A S E



Histograms represent CD86 surface marker expression. In each histogram there are four curves; an isotype control (grey dotted line), a non-stimulated moDCs -stated as UT (curve filled with grey colour), a positive control- the sample stimulated with LPS (100 ng/ml) (thick black line), and moDCs exposed to cGAMP (curve filled with black colour). The x-axis shows the fluorescence intensity of CD86-PE, and additionally, median fluorescence intensity of CD86 PE from each of the curve is shown in the form of numbers, stated as "X-med". The y-axis shows the percentage of cells in the gate. A-D represent data from replicate 1, from the lowest 0.2μl cGAMP concentration to the highest 100μl cGAMP; same for replicate 2 (E-H). For a better overview, data from histograms is plotted in the form of bar chart (I). Each column represents mean value of CD83 MFI collected from 2 replicates. Error bars indicate standard deviation between 2 replicates. P value was generated with ordinary one-way ANOVA test in Prism 6 program.

APPENDIX 9. DAY 6 CD86 SURFACE MARKER

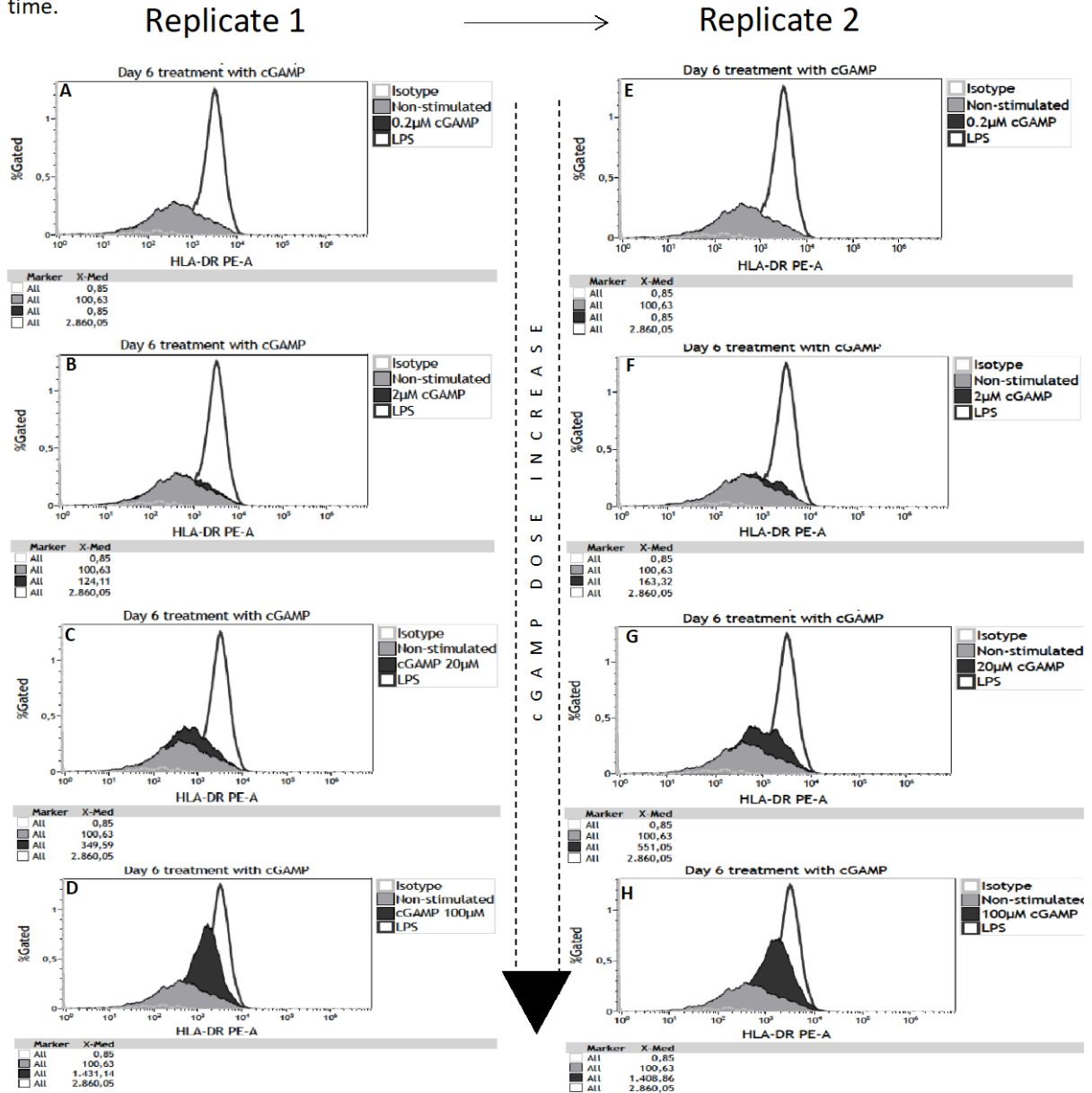
CD86 marker expression. DCs were exposed to different concentration of cGAMP on day 6 of incubation time. Each concentration was added in 2 replicates.



Histograms represent CD86 surface marker expression. In each histogram there are four curves; an isotype control (grey dotted line), a non-stimulated moDCs - stated as UT (curve filled with grey colour), a positive control- the sample stimulated with LPS (100 ng/ml) (thick black line), and moDCs exposed to cGAMP (curve filled with black colour). The x-axis shows the fluorescence intensity of CD86-PE, and additionally, median fluorescence intensity of CD86 PE from each of the curve is shown in the form of numbers, stated as "X-med". The y-axis shows the percentage of cells in the gate. A-D represent data from replicate 1, from the lowest 0.2μl cGAMP concentration to the highest 100μl cGAMP; same for replicate 2 (E-H). For a better overview, data from histograms is plotted in the form of bar chart (I). Each column represents mean value of CD83 MFI collected from 2 replicates. Error bars indicate standard deviation between 2 replicates. P value was generated with ordinary one-way ANOVA test in Prism 6 program.

APPENDIX 10. DAY 6 HLA-DR SURFACE EXPRESSION

HLA-DR marker expression. DCs were exposed to different concentration of cGAMP on day 6 of incubation time.

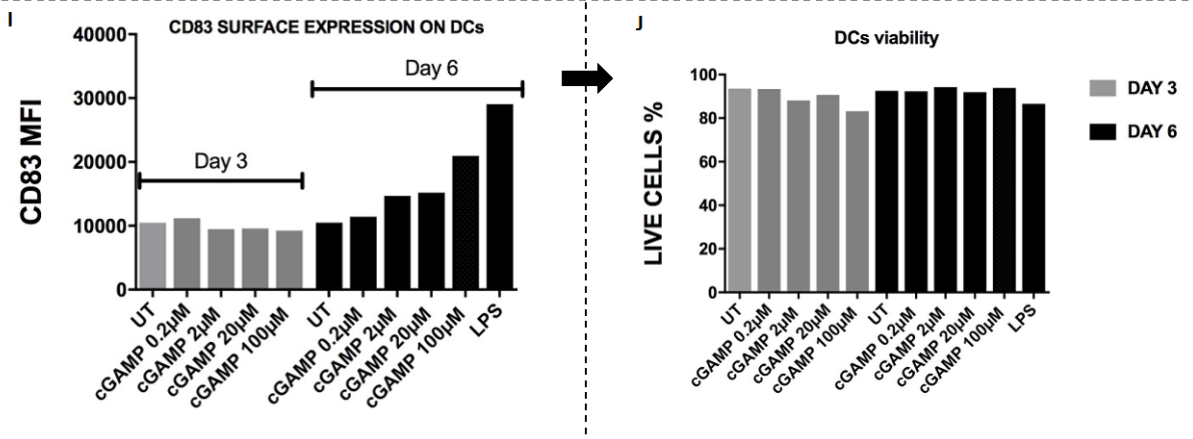
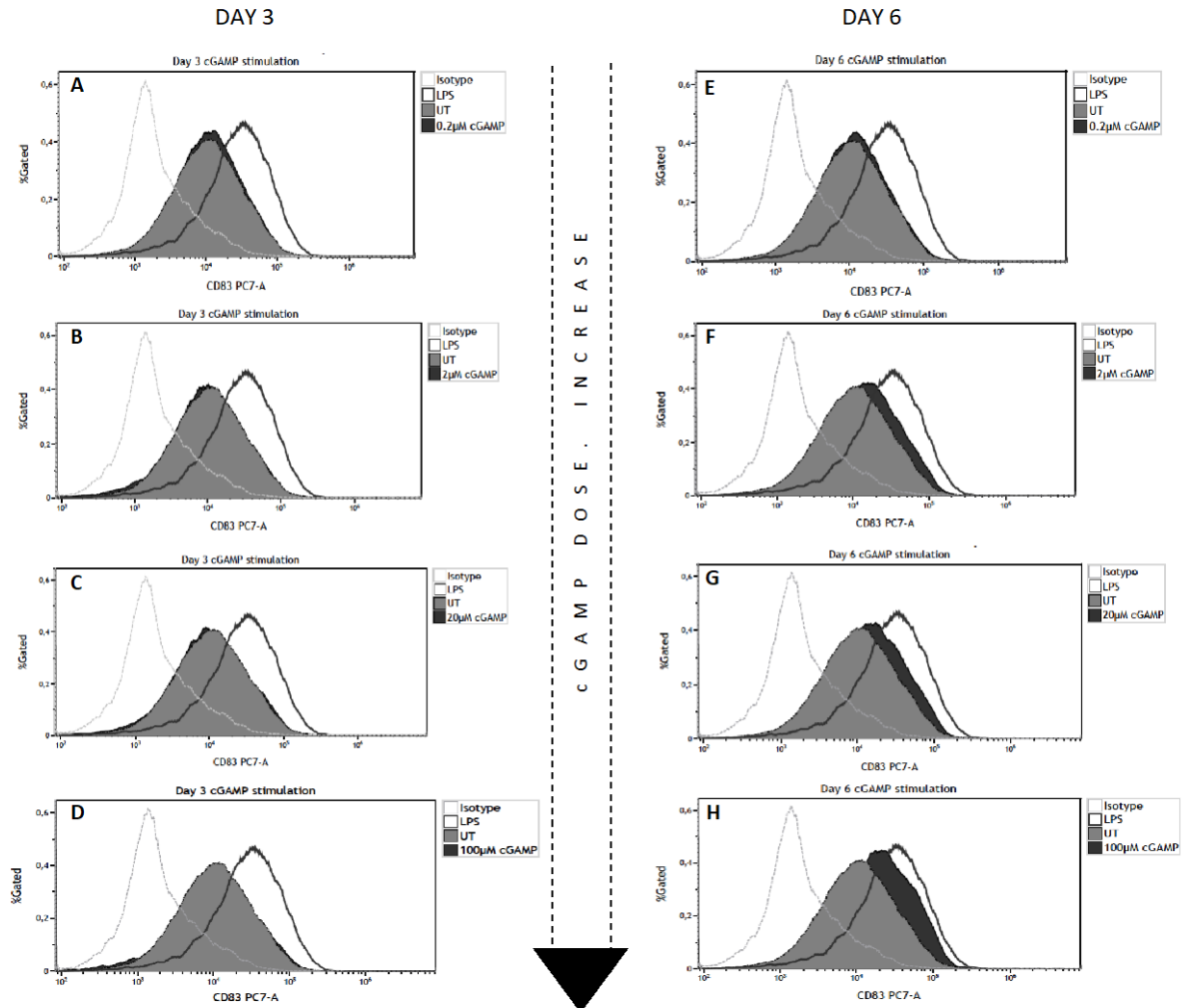


Histograms represent HLA-DR surface marker expression. In each histogram there are four curves; an isotype control (grey dotted line), a non-stimulated moDCs -stated as UT (curve filled with grey colour), a positive control- the sample stimulated with LPS (100 ng/ml) (thick black line), and moDCs exposed to cGAMP (curve filled with black colour). The x-axis shows the fluorescence intensity of CD86-PE, and additionally, median fluorescence intensity of CD86 PE from each of the curve is shown in the form of numbers, stated as "X-med". The y-axis shows the percentage of cells in the gate. A-D represent data from replicate 1, from the lowest 0.2 μl cGAMP concentration to the highest 100 μl cGAMP; same for replicate 2 (E-H). For a better overview, data from histograms is plotted in the form of bar chart (I). Each column represents mean value of HLA-DR MFI collected from 2 replicates. Error bars indicate standard deviation between 2 replicates. P value was generated with ordinary one-way ANOVA test in Prism 6 program.

It should be noted that there is no HLA-DR marker expression data provided for day 3 treatment with cGAMP due to lack of antibody.

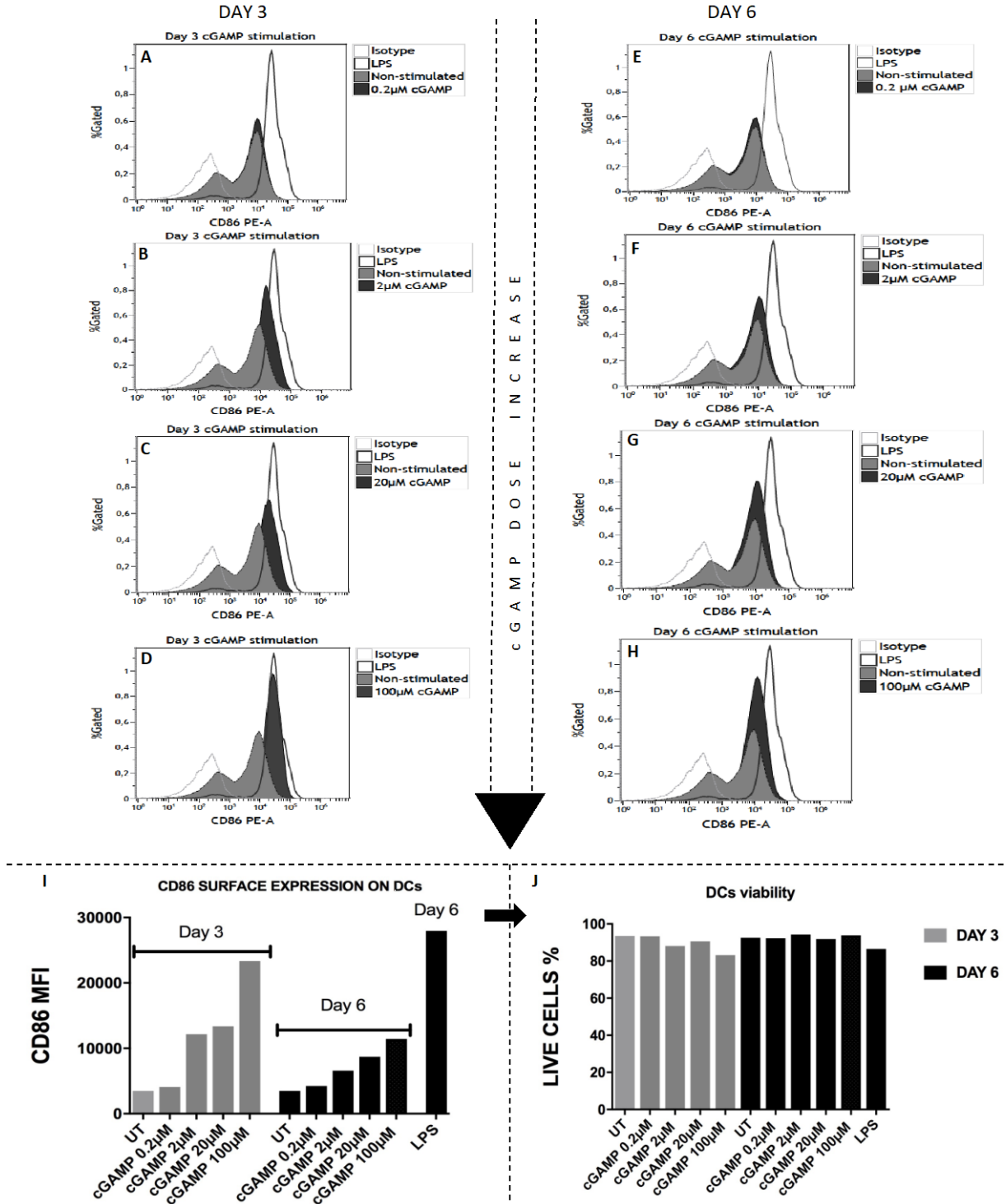
APPENDIX 11. cGAMP TITRATION EXPERIMENT. EFFECT OF DIFFERENT DOSES ON DCs MATURATION BASED ON THE EXPRESSION OF CD83 MARKER. cGAMP WAS ADDED ON DAY 3 OR ON DAY 6 OF INCUBATION TIME.

Histograms represent CD83 surface marker expression: A-D cGAMP added only on day 3, E-H cGAMP added only on day 6 of incubation time. For a better overview, data from histograms is plotted in the form of bar chart (I). DCs viability is represented in (J).

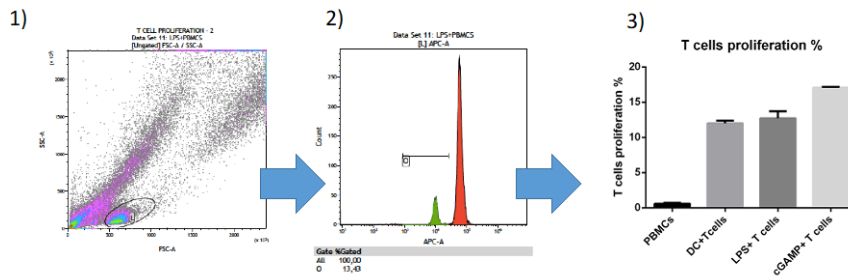


APPENDIX 12. cGAMP TITRATION EXPERIMENT. EFFECT OF DIFFERENT DOSES ON DCs MATURATION BASED ON THE EXPRESSION OF CD86 MARKER. cGAMP WAS ADDED ON DAY 3 OR ON DAY 6 OF INCUBATION TIME.

Histograms represent CD86 surface marker expression: A-D cGAMP added only on day 3, E-H cGAMP added only on day 6 of incubation time. For a better overview, bar chart (I) illustrates merged data from below histograms and replicates included in Appendix 1. DCs viability is represented in (J).

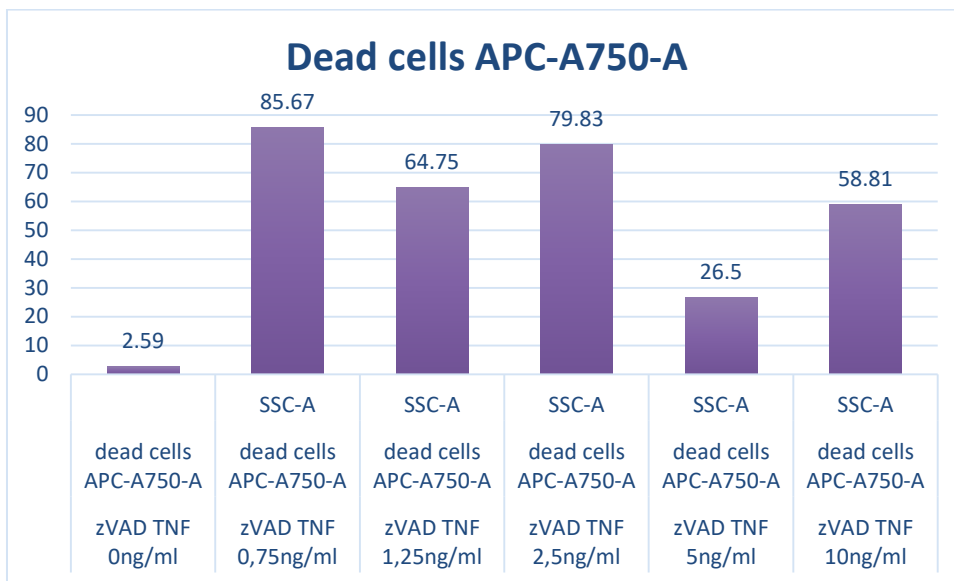


APPENDIX 13. GATEING FOR “T CELLS” POPULATION



1) Represents population of PBMCs, which have been stained for 1 cells characteristic markers: CD4 anti-human PerCP (clone OKT4) (BioLegend) and mouse anti-human CD8 Per-CP-Cy5.5™ (clone SK-1; CD8α specific) (BD Biosciences). T cells population is gated in the black circle 2) Represents proliferation status of the gated cells population based on the staining for cells proliferation, eFluor 670 intensity. 3) Interpretation of data from histograms in the form of bar charts.

APPENDIX 14. TREATMENT WITH LOWER DOSES OF TNF IN COMBINATION WITH zVAD, KILLED L929 CELLS.



X-axis represents treatment of L929 cells using lower doses of TNF with combination of zVAD. Y axis indicates % of dead cells.

Bibliography

- Aaes, T. L. *et al.* (2016) 'Vaccination with Necroptotic Cancer Cells Induces Efficient Anti-tumor Immunity', *Cell Reports*, 15(2), pp. 274–287. doi: 10.1016/j.celrep.2016.03.037.
- Ahn, J. *et al.* (2012) 'STING manifests self DNA-dependent inflammatory disease', *Proceedings of the National Academy of Sciences*, 109(47), pp. 19386–19391. doi: 10.1073/pnas.1215006109.
- Ahn, J. *et al.* (2014) 'Inflammation-driven carcinogenesis is mediated through STING', *Nature Communications*. doi: 10.1038/ncomms6166.
- Ahn, J. and Barber, G. N. (2014) 'Self-DNA, STING-dependent signaling and the origins of autoinflammatory disease', *Current Opinion in Immunology*, pp. 121–126. doi: 10.1016/j.coi.2014.10.009.
- Apetoh, L. *et al.* (2007) 'Toll-like receptor 4-dependent contribution of the immune system to anticancer chemotherapy and radiotherapy', *Nature Medicine*. doi: 10.1038/nm1622.
- Barber, G. N. (2015) 'STING: Infection, inflammation and cancer', *Nature Reviews Immunology*, pp. 760–770. doi: 10.1038/nri3921.
- Vanden Berghe, T. *et al.* (2015) 'Molecular crosstalk between apoptosis, necroptosis, and survival signaling', *Molecular & Cellular Oncology*, 2(4), p. e975093. doi: 10.4161/23723556.2014.975093.
- Chen, G. Y. and Nuñez, G. (2010) 'Sterile inflammation: Sensing and reacting to damage', *Nature Reviews Immunology*, pp. 826–837. doi: 10.1038/nri2873.
- Chen, X. *et al.* (2016) 'Pyroptosis is driven by non-selective gasdermin-D pore and its morphology is different from MLKL channel-mediated necroptosis', *Cell Research*. doi: 10.1038/cr.2016.100.
- Cho, Y., Challa, S. and Chan, F. K. M. (2011) 'A RNA interference screen identifies RIP3 as an essential inducer of TNF-induced programmed necrosis', in *Advances in Experimental Medicine and Biology*, pp. 589–593. doi: 10.1007/978-1-4419-6612-4_62.
- Deng, L. *et al.* (2014) 'STING-dependent cytosolic DNA sensing promotes radiation-induced type I interferon-dependent antitumor immunity in immunogenic tumors', *Immunity*. doi: 10.1016/j.immuni.2014.10.019.
- Ebrahimi, M. *et al.* (2009) 'Immediate exposure to TNF-alpha activate dendritic cells derived from non-purified cord blood mononuclear cells.', *Iranian journal of immunology : IJI*. doi: IJlv6i3A1.
- He, S. *et al.* (2009) 'Receptor Interacting Protein Kinase-3 Determines Cellular Necrotic Response to TNF- α ', *Cell*, 137(6), pp. 1100–1111. doi: 10.1016/j.cell.2009.05.021.
- Ishikawa, H., Ma, Z. and Barber, G. N. (2009) 'STING regulates intracellular DNA-mediated, type I interferon-dependent innate immunity', *Nature*, 461(7265), pp. 788–792. doi: 10.1038/nature08476.
- Klarquist, J. *et al.* (2014) 'STING-Mediated DNA Sensing Promotes Antitumor and Autoimmune Responses to Dying Cells', *The Journal of Immunology*, 193(12), pp. 6124–6134. doi: 10.4049/jimmunol.1401869.
- Koo, G. B. *et al.* (2015) 'Methylation-dependent loss of RIP3 expression in cancer represses programmed necrosis in response to chemotherapeutics', *Cell Research*. doi: 10.1038/cr.2015.56.

- Krysko, D. V. *et al.* (2006) 'Macrophages use different internalization mechanisms to clear apoptotic and necrotic cells', *Cell Death and Differentiation*. doi: 10.1038/sj.cdd.4401900.
- Lee, B. L. and Barton, G. M. (2014) 'Trafficking of endosomal Toll-like receptors', *Trends in Cell Biology*, pp. 360–369. doi: 10.1016/j.tcb.2013.12.002.
- Li, T. *et al.* (2016) 'Antitumor Activity of cGAMP via Stimulation of cGAS-cGAMP-STING-IRF3 Mediated Innate Immune Response', *Scientific Reports*. doi: 10.1038/srep19049.
- Maeda, A. and Fadeel, B. (2014) 'Mitochondria released by cells undergoing TNF- α -induced necroptosis act as danger signals', *Cell Death and Disease*. doi: 10.1038/cddis.2014.277.
- Moreno-Gonzalez, G., Vandenabeele, P. and Krysko, D. V. (2016) 'Necroptosis: A novel cell death modality and its potential relevance for critical care medicine', *American Journal of Respiratory and Critical Care Medicine*, pp. 415–428. doi: 10.1164/rccm.201510-2106CI.
- Moriwaki, K. *et al.* (2015) 'Differential roles of RIPK1 and RIPK3 in TNF-induced necroptosis and chemotherapeutic agent-induced cell death', *Cell Death and Disease*. doi: 10.1038/cddis.2015.16.
- Moujalled, D. M. *et al.* (2013) 'TNF can activate RIPK3 and cause programmed necrosis in the absence of RIPK1.', *Cell death & disease*. doi: 10.1038/cddis.2012.201.
- Ng, K. W. *et al.* (2018) 'cGAS–STING and Cancer: Dichotomous Roles in Tumor Immunity and Development', *Trends in Immunology*, pp. 44–54. doi: 10.1016/j.it.2017.07.013.
- Pecorino, L. (2012) 'Introduction', in *Molecular biology of cancer : mechanisms, targets, and therapeutics*, pp. 1–16. Available at: https://books.google.ie/books?id=tl_vcU85QU4C&pg=PA2&lpg=PA2&dq='Cancer+is+a+group+of+diseases+characterized+by+unregulated+cell+growth+and+the+invasion+and+spread+of+cells+from+the+site+of+origin,+or+primary+site,+to+other+sites+in+the+body'&source=bl&ot.
- Saitoh, T. *et al.* (2009) 'Atg9a controls dsDNA-driven dynamic translocation of STING and the innate immune response', *Proceedings of the National Academy of Sciences*, 106(49), pp. 20842–20846. doi: 10.1073/pnas.0911267106.
- Škrnjug, I., Guzmán, C. A. and Ruecker, C. (2014) 'Cyclic GMP-AMP displays mucosal adjuvant activity in mice', *PLoS ONE*, 9(10). doi: 10.1371/journal.pone.0110150.
- Sun, L. *et al.* (2013) 'Cyclic GMP-AMP synthase is a cytosolic DNA sensor that activates the type I interferon pathway', *Science*, 339(6121), pp. 786–791. doi: 10.1126/science.1232458.
- Vandenabeele, P. *et al.* (2010) 'Molecular mechanisms of necroptosis: An ordered cellular explosion', *Nature Reviews Molecular Cell Biology*, pp. 700–714. doi: 10.1038/nrm2970.
- Vanlangenakker, N. *et al.* (2011) 'TNF-induced necroptosis in L929 cells is tightly regulated by multiple TNFR1 complex I and II members', *Cell Death and Disease*. doi: 10.1038/cddis.2011.111.
- Vercammen, D. *et al.* (1998) 'Inhibition of Caspases Increases the Sensitivity of L929 Cells to Necrosis Mediated by Tumor Necrosis Factor', *The Journal of Experimental Medicine*. doi: 10.1084/jem.187.9.1477.
- Woo, S. R. *et al.* (2014) 'STING-dependent cytosolic DNA sensing mediates innate immune recognition of immunogenic tumors', *Immunity*, 41(5), pp. 830–842. doi: 10.1016/j.immuni.2014.10.017.

Wu, J. *et al.* (2013) 'Cyclic GMP-AMP is an endogenous second messenger in innate immune signaling by cytosolic DNA', *Science*, 339(6121), pp. 826–830. doi: 10.1126/science.1229963.

Wu, W., Liu, P. and Li, J. (2012) 'Necroptosis: An emerging form of programmed cell death', *Critical Reviews in Oncology/Hematology*, pp. 249–258. doi: 10.1016/j.critrevonc.2011.08.004.

Zarif, J. C. *et al.* (2016) 'A phased strategy to differentiate human CD14+ monocytes into classically and alternatively activated macrophages and dendritic cells', *BioTechniques*. doi: 10.2144/000114435.